NBER WORKING PAPER SERIES

# VALUING THE GLOBAL MORTALITY CONSEQUENCES OF CLIMATE CHANGE ACCOUNTING FOR ADAPTATION COSTS AND BENEFITS

Tamma A. Carleton
Amir Jina
Michael T. Delgado
Michael Greenstone
Trevor Houser
Solomon M. Hsiang
Andrew Hultgren
Robert E. Kopp
Kelly E. McCusker
Ishan B. Nath
James Rising
Ashwin Rode
Hee Kwon Seo
Arvid Viaene
Jiacan Yuan
Alice Tianbo Zhang

Working Paper 27599
http://www.nber.org/papers/w27599

NATIONAL BUREAU OF ECONOMIC RESEARCH
1050 Massachusetts Avenue
Cambridge, MA 02138
July 2020, Revised August 2021

This project is an output of the Climate Impact Lab that gratefully acknowledges funding from the Energy Policy Institute of Chicago (EPIC), International Growth Centre, National Science Foundation, Sloan Foundation, Carnegie Corporation, and Tata Center for Development. Tamma Carleton acknowledges funding from the US Environmental Protection Agency Science To Achieve Results Fellowship (#FP91780401). We thank Trinetta Chong, Greg Dobbels, Diana Gergel, Radhika Goyal, Simon Greenhill, Hannah Hess, Dylan Hogan, Azhar Hussain, Stefan Klos, Theodor Kulczycki, Brewster Malevich, Sébastien Annan Phan, Justin Simcock, Emile Tenezakis, Jingyuan Wang, and Jong-kai Yang for invaluable research assistance during all stages of this project, and Megan Landín, Terin Mayer, and Jack Chang for excellent project management. We thank David Anthoff, Max Auffhammer, Olivier Deschênes, Avi Ebenstein, Nolan Miller, Wolfram Schlenker, and numerous workshop participants at University of Chicago, Stanford, Princeton, UC Berkeley, UC San Diego, UC Santa Barbara, University of Pennsylvania, University of San Francisco, University of Virginia, University of Wisconsin-Madison, University of Minnesota Twin Cities, NBER Summer Institute, LSE, PIK, Oslo University, University of British Columbia, Gothenburg University, the European Center for Advanced Research in Economics and Statistics, the National Academies of Sciences, and the Econometric Society for comments, suggestions, and help with data. The views expressed herein are those of the authors and do not necessarily reflect the views of the National Bureau of Economic Research.

Valuing the Global Mortality Consequences of Climate Change Accounting for Adaptation Costs and Benefits

Tamma A. Carleton, Amir Jina, Michael T. Delgado, Michael Greenstone, Trevor Houser, Solomon M. Hsiang, Andrew Hultgren, Robert E. Kopp, Kelly E. McCusker, Ishan B. Nath, James Rising, Ashwin Rode, Hee Kwon Seo, Arvid Viaene, Jiacan Yuan, and Alice Tianbo Zhang

NBER Working Paper No. 27599
July 2020, Revised August 2021
JEL No. Q54

## ABSTRACT

Using 40 countries' subnational data, we estimate age-specific mortality-temperature relationships and extrapolate them to countries without data today and into a future with climate change. We uncover a U-shaped relationship where extreme cold and hot temperatures increase mortality rates, especially for the elderly. Critically, this relationship is flattened by both higher incomes and adaptation to local climate. Using a revealed preference approach to recover unobserved adaptation costs, we estimate that the mean global increase in mortality risk due to climate change, accounting for adaptation benefits and costs, is valued at roughly 3.2% of global GDP in 2100 under a high emissions scenario. Notably, today's cold locations are projected to benefit, while today's poor and hot locations have large projected damages. Finally, our central estimates indicate that the release of an additional ton of CO2 today will cause mortality-related damages of $36.6 under a high emissions scenario and using a 2% discount rate, with an interquartile range accounting for both econometric and climate uncertainty of [-$7.8, $73.0]. Under a moderate emissions scenario, these damages are valued at $17.1 [-$24.7, $53.6]. These empirically grounded estimates exceed the previous literature's estimates by an order of magnitude.

Tamma A. Carleton
Bren School of Environmental
Science & Management
University of California, Santa Barbara
Santa Barbara, CA 93106
tcarleton@uchicago.edu

Amir Jina
Harris School of Public Policy
University of Chicago
1155 East 60th Street
Chicago, IL 60637
and NBER
amirjina@uchicago.edu

Michael T. Delgado
Rhodium Group
647 4th St.
Oakland, CA 94607
mdelgado@rhg.com

Michael Greenstone
University of Chicago
Department of Economics
1126 E. 59th Street
Chicago, IL 60637
and NBER
mgreenst@uchicago.edu

Trevor Houser
Rhodium Group
647 4th St.
Oakland, CA 94607
tghouser@rhg.com

Solomon M. Hsiang
Goldman School of Public Policy
University of California, Berkeley
2607 Hearst Avenue
Berkeley, CA 94720-7320
and NBER
shsiang@berkeley.edu

Andrew Hultgren
University of California at Berkeley
hultgren@berkeley.edu

Robert E. Kopp
Department of Earth and Planetary Sciences
Wright Labs, 610 Taylor Road
Rutgers University
Piscataway, NJ 08854-8066
Robert.Kopp@rutgers.edu

Kelly E. McCusker
Rhodium Group
647 4th Street
Oakland, CA 94607
kmccusker@rhg.com

Ishan B. Nath
Department of Economics
University of Chicago
1126 E. 59th St.
Chicago, IL 60637
inath@uchicago.edu

James Rising
Grantham Research Institute
London School of Economics
London, UK
jarising@gmail.com

Ashwin Rode
Department of Economics
University of Chicago
1126 E. 59th St.
Chicago, IL 60637
aarode@uchicago.edu

Hee Kwon Seo
University of Chicago
Booth School of Business
5807 S. Woodlawn Ave.
Chicago, IL 60637
hkseo@chicagobooth.edu

Arvid Viaene
E.CA Economics
Brussels, Belgium
arvid.viaene.db@gmail.com

Jiacan Yuan
Department of Atmospheric
and Oceanic Sciences
Fudan University
Shanghai, China
jiacan.yuan@gmail.com

Alice Tianbo Zhang
Department of Economics
Williams School of Commerce,
Economics, and Politics
Washington and Lee University
Huntley 304
Lexington, VA 24450
atzhang@wlu.edu

An online appendix is available at http://www.nber.org/data-appendix/w27599

# 1 Introduction

Understanding the likely global economic impacts of climate change is of tremendous practical value to both policymakers and researchers. On the policy side, decisions are currently made with incomplete and inconsistent information on the benefits of greenhouse gas emissions reductions. These inconsistencies are reflected in global climate policy, which is at once both lenient and wildly inconsistent. To date, the economics literature has struggled to mitigate this uncertainty, lacking empirically founded and globally comprehensive estimates of the total burden imposed by climate change that account for the benefits and costs of adaptation. This problem is made all the more difficult because emissions today influence the global climate for hundreds of years. Thus, any reliable estimate of the damage from climate change must include projections of economic impacts that are both long-run and at global scale.

Decades of study have accumulated numerous theoretical and empirical insights and important findings regarding the economics of climate change, but a fundamental gulf persists between the two main types of analyses. On the one hand, there are stylized models able to capture the multi-century and global nature of climate change, such as "integrated assessment models" (IAMs) (e.g., Nordhaus, 1992; Tol, 1997; Stern, 2006); their great appeal is that they provide an answer to the question of what the global costs of climate change will be. However, IAMs require many assumptions and this weakens the authority of their answers. On the other hand, there has been an explosion of highly resolved empirical analyses whose credibility lies in their use of real world data and careful econometric measurement (e.g., Schlenker and Roberts, 2009; Deschênes and Greenstone, 2007). Yet these analyses tend to be limited in geographic extent and/or rely on short-run changes in weather that are unlikely to fully account for adaptation to gradual climate change (Hsiang, 2016). At its core, this dichotomy persists because researchers have traded off between being complete in scale and scope or investing heavily in data collection and analysis.

This paper aims to resolve the tension between these approaches by providing empirically-derived estimates of climate change's impacts on global mortality risk. Importantly, these estimates are at the scale of IAMs, yet grounded in detailed econometric analyses using high-resolution globally representative data, and account for adaptation to gradual climate change. The analysis proceeds in three steps that lead to the paper's three main findings.

First, we estimate regressions to infer age-specific mortality-temperature relationships using historical data. These regressions are fit on the most comprehensive dataset ever collected on annual, subnational mortality statistics from 40 countries that cover 38% of the global population. The benefits of adaptation to climate change and the benefits of projected future income growth are estimated by allowing the mortality-temperature response function to vary with long-run climate (e.g., Auffhammer, 2018) and income per capita (e.g., Fetzer, 2014). This modeling of heterogeneity allows us to predict the structure of the mortality-temperature relationship across locations where we lack mortality data, yielding estimates for the entire world.

These regressions uncover a plausibly causal U-shaped relationship where extremely cold and hot temperatures increase mortality rates, especially for those aged 65 and older. Moreover, this relationship is quite heterogeneous across the planet: we find that both income and long-run climate substantially moderate mor-

tality sensitivity to temperature. When we combine these results with current global data on climate, income, and population, we find that the effect of an additional very hot day (35°C / 95°F) on mortality in the >64 age group is ∼50% larger in regions of the world where mortality data are unavailable. This finding suggests that prior estimates may understate climate change impacts, because they disproportionately rely on data from wealthy economies and temperate climates. However, we note that because modern populations have not experienced multiple alternative climates, the estimates of heterogeneity rely on cross-sectional variation and they must be considered associational.

Second, we combine the regression results with standard future predictions of climate, income and population to project future climate change-induced mortality risk both in terms of fatality rates and its monetized value. The paper's mean estimate of the projected increase in the global mortality rate due to climate change is 73 deaths per 100,000 at the end of the century under a high emissions scenario (i.e., Representative Concentration Pathway (RCP) 8.5), with an interquartile range of [6, 101] due both to econometric and climate uncertainty. This effect is similar in magnitude to the current global mortality burden of all cancers or all infectious diseases. It is noteworthy that these impacts are predicted to be unequally distributed across the globe: for example, mortality rates in Accra, Ghana are projected to increase by 17% at the end of the century under a high emissions scenario, while in London, England, mortality rates are projected to decrease by 8% due to milder winters. Importantly, a failure to account for climate adaptation and the benefits of income growth would lead to overstating the mortality costs of climate change by a factor of about 3.

Of course, adaptation is costly; we develop a stylized revealed preference model that leverages observed differences in temperature sensitivity across space to infer these costs. When monetizing projected deaths due to climate change with the value of a statistical life (VSL) and adding the estimated costs of adaptation, the total mortality burden of climate change is equal to roughly 3.2% of global GDP at the end of the century under a high emissions scenario. We find that poor countries are projected to disproportionately experience impacts through deaths, while wealthy countries experience impacts largely through costly adaptation investments.

Third, we use these estimates to compute the global marginal willingness-to-pay (MWTP) to avoid the alteration of mortality risk associated with the temperature change from the release of an additional metric ton of $CO_2$. We call this the excess mortality "partial" social cost of carbon (SCC); a "full" SCC would encompass impacts across all affected outcomes. Our estimates imply that the excess mortality partial SCC is roughly \$36.6 [-\$7.8, \$73.0] (in 2019 USD) with a high emissions scenario (RCP8.5) under a 2% discount rate and using an age-varying VSL. This value falls to \$17.1 [-\$24.7, \$53.6] with a moderate emissions scenario (RCP4.5). The excess mortality partial SCC is lower in this scenario because the relationship between mortality risk and temperature is convex, meaning that marginal damages are greater under higher baseline emissions.

Overall, this paper's results suggest that the temperature related mortality risk from climate change is substantially greater than previously understood. For example, the estimated mortality partial SCC is more than an order of magnitude larger than the partial SCC for all health impacts embedded in the FUND IAM. Further, under the high emissions scenario, the estimated excess mortality partial SCC is ∼72% of the Biden

Administration's *full* interim SCC.[1]

In generating these results, this paper overcomes multiple challenges that have plagued the previous literature. The first challenge is that $CO_2$ is a global pollutant, so it is necessary to account for the heterogeneous costs of climate change across the entire planet. The second challenge is that today, there is substantial adaptation to climate, as people successfully live in both Houston, TX and Anchorage, AK, and climate change will undoubtedly lead to new adaptations in the future. The extent to which investments in adaptation can limit the impacts of climate change is a critical component of damage estimates. We address both of these challenges by combining extensive data with an econometric approach that models heterogeneity in the mortality-temperature relationship, allowing us to predict mortality-temperature relationships at high resolution globally and into the future as climate and incomes evolve. Specifically, we develop estimates of climate change impacts at high resolution, effectively allowing for 24,378 representative agents. In contrast, the previous literature has assumed the world is comprised of, at maximum, 170 heterogenous regions (Burke, Hsiang, and Miguel, 2015), but typically far fewer (Nordhaus and Yang, 1996; Tol, 1997).

A final challenge is that adaptation responses are costly, and these costs must be accounted for in a full assessment of climate change impacts. While our revealed preference approach to inferring adaptation costs relies on a strong set of simplifying assumptions, it can be directly estimated with available data and represents an important advance on previous literature, which has either quantified adaptation benefits without estimating costs (e.g., Heutel, Miller, and Molitor, 2017) or tried to measure the costs of individual adaptive investments in selected locations (e.g., Barreca et al., 2016), an approach that is poorly equipped to capture the wide range of potential responses to warming.

The rest of this paper is organized as follows: Section 2 provides definitions and some basic intuition for the economics of adaptation to climate change in the context of mortality. Section 3 details data used throughout the analysis. Section 4 describes our empirical model and estimations results. Section 5 presents projections of climate change impacts with and without the benefits of adaptation. Section 6 outlines a revealed preference approach that allows us to infer adaptation costs and uses this framework to present empirically-derived projections of the mortality risk of climate change accounting for the costs and benefits of adaptation. Section 7 constructs a partial SCC, Section 8 discusses key limitations of the analysis, and Section 9 concludes.

## 2 Conceptual framework

This section sets out a simple conceptual framework that guides the empirical model the paper uses to estimate society's willingness to pay (WTP) to avoid the mortality risks from climate change. In estimating these mortality risks, it is critical to account for individuals' compensatory responses, or adaptations, to climate change, such as investments in air conditioning. These adaptations have both benefits that reduce the risks of extreme temperatures and costs in the form of foregone consumption. Thus, the full mortality risk of climate change is the sum of changes in mortality rates after accounting for adaptation and the costs

[1]This comparison is made using our preferred valuation scenario, which includes an age-adjusted VSL and a discount rate of 2%. The Biden Administration's interim SCC uses a 3% discount rate and an age-invariant VSL. Under these valuation assumptions, the estimated excess mortality partial SCC is 44% of the Biden Administration's full interim SCC.

of those adaptations. Here, we define some key objects that the paper will estimate, including the full value of mortality risk due to climate change.

We define the *climate* as the joint probability distribution over a vector of possible conditions that can be expected to occur over a specific interval of time. Following the notation of Hsiang (2016), let $\boldsymbol{C}$ be a vector of parameters describing the entire joint probability distribution over all relevant climatic variables (e.g., $\boldsymbol{C}$ might contain the mean and variance of daily average temperature and rainfall, among other parameters). We define weather realizations as a random vector $\boldsymbol{c}$ drawn from a distribution characterized by $\boldsymbol{C}$. Mortality risk is a function of both weather $\boldsymbol{c}$ and a composite good $\boldsymbol{b} = \xi(b_1, ..., b_K)$ comprising all choice variables $b_k$ that could influence mortality risk, such as installation of air conditioning and time allocated to indoor activities. The endogenous choices in $\boldsymbol{b}$ are the outcome of a stylized model in which individuals maximize expected utility by trading off consumption of a numeraire good and $\boldsymbol{b}$, subject to a budget constraint, as outlined in detail in Section 6. Mortality risk is then captured by the probability of death $f = f(\boldsymbol{b}, \boldsymbol{c})$.

Climate change will influence mortality risk through two pathways.[2] First, a change in $\boldsymbol{C}$ will directly alter realized weather draws, changing $\boldsymbol{c}$. Second, a change in $\boldsymbol{C}$ can alter individuals' beliefs about their likely weather realizations, shifting how they act, and ultimately changing their endogenous choice variables $\boldsymbol{b}$. Endogenous adjustments to $\boldsymbol{b}$ therefore capture all long-run adaptation to the climate (e.g., Mendelsohn, Nordhaus, and Shaw, 1994; Kelly, Kolstad, and Mitchell, 2005). Since the climate $\boldsymbol{C}$ determines both $\boldsymbol{c}$ and $\boldsymbol{b}$, the probability of death at an initial climate $\boldsymbol{C}_{t_0}$ is written as:

$$\Pr(\text{death} \mid \boldsymbol{C}_{t_0}) = f(\boldsymbol{b}(\boldsymbol{C}_{t_0}), \boldsymbol{c}(\boldsymbol{C}_{t_0})), \tag{1}$$

where $\boldsymbol{c}(\boldsymbol{C})$ is a random vector $\boldsymbol{c}$ drawn from the distribution characterized by $\boldsymbol{C}$.

Many previous empirical estimates assume that individuals do not make any adaptations or compensatory responses to an altered climate (e.g., Deschênes and Greenstone, 2007; Houser et al., 2015). Under this approach, the change in mortality risk incurred due to a change in climate from $\boldsymbol{C}_{t_0}$ to $\boldsymbol{C}_t$ is calculated as:

$$\textit{mortality effects of climate change without adaptation} = f(\boldsymbol{b}(\boldsymbol{C}_{t_0}), \boldsymbol{c}(\boldsymbol{C}_t)) - f(\boldsymbol{b}(\boldsymbol{C}_{t_0}), \boldsymbol{c}(\boldsymbol{C}_{t_0})), \tag{2}$$

which ignores the fact that individuals will choose new values of $\boldsymbol{b}$ as their beliefs about $\boldsymbol{C}$ evolve.

A more realistic estimate for the change in mortality due to a change in climate is:

$$\textit{mortality effects of climate change with adaptation} = f(\boldsymbol{b}(\boldsymbol{C}_t), \boldsymbol{c}(\boldsymbol{C}_t)) - f(\boldsymbol{b}(\boldsymbol{C}_{t_0}), \boldsymbol{c}(\boldsymbol{C}_{t_0})). \tag{3}$$

If the climate is changing such that the mortality risk from $\boldsymbol{C}_t$ is higher than $\boldsymbol{C}_{t_0}$ when holding $\boldsymbol{b}$ fixed, then the endogenous adjustment of $\boldsymbol{b}$ will generate benefits of adaptation weakly greater than zero, since these damages may be partially mitigated. In practice, the sign of the difference between Equations 2 and 3 will depend on the degree to which climate change reduces extremely cold days versus increases extremely hot days, and the optimal adaptation that agents undertake in response to these competing changes.

Several analyses have estimated reduced-form versions of Equation 3, confirming that accounting for

[2] Hsiang (2016) describes these two channels as a "direct effect" and a "belief effect."

endogenous changes to technology, behavior, and investment mitigates the direct effects of climate in a variety of contexts (e.g., Barreca et al., 2016).[3] Importantly, however, while this approach accounts for the *benefits* of adaptation, it does not account for its *costs*. If adjustments to $\boldsymbol{b}$ were costless and provided protection against the climate, then we would expect universal uptake of highly adapted values for $\boldsymbol{b}$ so that temperature would have no effect on mortality. But we do not observe this to be true: for example, Heutel, Miller, and Molitor (2017) find that the mortality effects of extremely hot days in warmer climates (e.g., Houston) are much smaller than in more temperature climates (e.g., Seattle).[4] We denote the costs of achieving adaptation level $\boldsymbol{b}$ as $A(\boldsymbol{b})$, measured in dollars of forgone consumption.

A full measure of the economic burden of climate change must account not only for the benefits generated by compensatory responses to these changes, but also their cost. Thus, the total cost of changing mortality risks that result from a climate change $\boldsymbol{C}_{t_0} \rightarrow \boldsymbol{C}_t$ is:

$$\textit{full value of mortality risk due to climate change} = VSL \underbrace{[f(\boldsymbol{b}(\boldsymbol{C}_t), \boldsymbol{c}(\boldsymbol{C}_t)) - f(\boldsymbol{b}(\boldsymbol{C}_{t_0}), \boldsymbol{c}(\boldsymbol{C}_{t_0}))]}_{\text{observable change in mortality rate}} + \underbrace{A(\boldsymbol{b}(\boldsymbol{C}_t)) - A(\boldsymbol{b}(\boldsymbol{C}_{t_0}))}_{\text{adaptation costs}}, \tag{4}$$

where $VSL$ is the value of a statistical life. It is apparent that omitting the costs of adaptation, $A(\boldsymbol{b})$, would lead to an incomplete measure of the full costs of mortality risk due to climate change.

This paper develops an empirical model to quantify climate change's impact on mortality risk at global scale, accounting for the benefits of adaptation, consistent with Equation 3. Throughout the analysis, we consider the effects of climate change induced changes in daily average temperature, such that the mortality risk of climate change implies effects of temperature only (as opposed to other climate variables, such as precipitation). Because income may also influence the choice variables in $\boldsymbol{b}$, we include the benefits of income growth in this empirical model, in addition to the benefits of climate adaptation. This empirical approach and the resulting climate change impact projections are detailed in Sections 4 and 5, respectively.

However, an empirical estimation of the full value of mortality risk due to climate change, shown in Equation 4, is more difficult, as total changes in adaptation costs between time periods cannot be observed directly. In principle, data on each adaptive action could be gathered and modeled (e.g., Deschênes and Greenstone, 2011), but since there exists an enormous number of possible adaptive margins that together make up the vector $\boldsymbol{b}$, computing the full cost of climate change using such an enumerative approach quickly becomes intractable. To make progress on quantifying the full value of mortality risk due to climate change, we develop a stylized revealed preference approach that leverages observed differences in climate sensitivity across locations to infer adaptation costs associated with the mortality risk from climate change. This approach, and resulting estimates of the full (monetized) value of the mortality risk due to climate change, are reported in Section 6.

Section 7 uses these estimates to compute the global marginal willingness-to-pay (MWTP) to avoid the alteration of mortality risk associated with the release of an additional metric ton of $CO_2$. We call this the

[3] For additional examples, see Schlenker and Roberts (2009); Hsiang and Narita (2012); Hsiang and Jina (2014); Barreca et al. (2015); Heutel, Miller, and Molitor (2017); Auffhammer (2018).

[4] Carleton and Hsiang (2016) document that such wedges in observed sensitivities to climate—which they call "adaptation gaps"—are a pervasive feature of the broader climate damages literature.

excess mortality "partial" social cost of carbon (SCC); a "full" SCC would encompass impacts across all affected sectors (e.g., labor productivity, damages from sea level rise, etc.).

# 3 Data

To estimate the mortality risks of climate change at global scale, we assemble a novel dataset composed of rich historical mortality records, high-resolution historical climate data, and future projections of climate, population, and income across the globe. Section 3.1 describes the data necessary to estimate $f(\boldsymbol{b}, \boldsymbol{c})$, the relationship between mortality and temperature, accounting for differences in climate and income. Section 3.2 outlines the data we use to predict the mortality-temperature relationship across the entire planet today and project its evolution into the future as populations adapt to climate change. Appendix B provides a more extensive description of each of these datasets.

## 3.1 Data to estimate the mortality-temperature relationship

### 3.1.1 Mortality data

Our mortality data are collected independently from 40 countries.[5] Combined, this dataset covers mortality outcomes for 38% of the global population, representing a substantial increase in coverage relative to existing literature; prior studies investigate an individual country (e.g., Burgess et al., 2017) or region (e.g., Deschenes, 2018), or combine small nonrandom samples from across multiple countries (e.g., Gasparrini et al., 2015). Table 1 summarizes each dataset, while spatial coverage, resolution, and temporal coverage are shown in Figure B1. We harmonize all records into a single multi-country unbalanced panel dataset of age-specific annual mortality rates, using three age categories: <5, 5-64, and >64, where the unit of observation is ADM2 (e.g., a county in the U.S.) by year.

### 3.1.2 Historical climate data

The analysis is performed with two separate groups of historical data on precipitation and temperature. First, we use the Global Meteorological Forcing Dataset (GMFD) (Sheffield, Goteti, and Wood, 2006), which relies on a weather model in combination with observational data. Second, we repeat our analysis with climate datasets that strictly interpolate observational data across space onto grids, combining temperature data from the daily Berkeley Earth Surface Temperature dataset (BEST) (Rohde et al., 2013) with precipitation data from the monthly University of Delaware dataset (UDEL) (Matsuura and Willmott, 2007). Table 1 summarizes these data; full data descriptions are provided in Appendix B.2. We link climate and mortality data by aggregating gridded daily temperature data to the annual measures at the same administrative level as the mortality records (i.e., ADM2) using a procedure detailed in Appendix B.2.4 that allows for the recovery of potential nonlinearities in the mortality-temperature relationship.

[5] We additionally use data from India as cross-validation of our main results, as the India data do not have records of age-specific mortality rates. The inclusion of India increases our data coverage to 55% of the global population.

**Table 1: Historical mortality & climate data**

***Mortality records***

| Country | N | Spatial scale[×] | Years | Age categories | Average annual mortality rate[*†] All-age | >64 yr. | Global pop. share[◇] | Average covariate values[*□] GDP per capita[⊗] | Avg. daily temp.[⊘] | Annual avg. days $> 28°C$ |
|---|---|---|---|---|---|---|---|---|---|---|
| Brazil | 228,762 | ADM2 | 1997-2010 | <5, 5-64, >64 | 525 | 4,096 | 0.028 | 11,192 | 23.8 | 35.2 |
| Chile | 14,238 | ADM2 | 1997-2010 | <5, 5-64, >64 | 554 | 4,178 | 0.002 | 14,578 | 14.3 | 0 |
| China | 7,488 | ADM2 | 1991-2010 | <5, 5-64, >64 | 635 | 7,507 | 0.193 | 4,875 | 15.1 | 25.2 |
| EU | 13,013 | NUTS2[‡] | 1990[▷]-2010 | <5, 5-64, >64 | 1,014 | 5,243 | 0.063 | 22,941 | 11.2 | 1.6 |
| France[⊕] | 3,744 | ADM2 | 1998-2010 | 0-19, 20-64, >64 | 961 | 3,576 | 0.009 | 31,432 | 11.9 | 0.3 |
| India[^] | 12,505 | ADM2 | 1957-2001 | All-age | 724 | – | 0.178 | 1,355 | 25.8 | 131.4 |
| Japan | 5,076 | ADM1 | 1975-2010 | <5, 5-64, >64 | 788 | 4,135 | 0.018 | 23,241 | 14.3 | 8.3 |
| Mexico | 146,835 | ADM2 | 1990-2010 | <5, 5-64,>64 | 561 | 4,241 | 0.017 | 16,518 | 19.1 | 24.6 |
| USA | 401,542 | ADM2 | 1968-2010 | <5, 5-64, >64 | 1,011 | 5,251 | 0.045 | 30,718 | 13 | 9.5 |
| **All Countries** | **833,203** | – | – | – | **780** | **4,736** | **0.554** | **20,590** | **15.5** | **32.6** |

***Historical climate datasets***

| Dataset | Citation | Method | Resolution | Variable | Source |
|---|---|---|---|---|---|
| GMFD, V1 | Sheffield, Goteti, and Wood (2006) | Reanalysis & Interpolation | 0.25° | temp. & precip. | Princeton University |
| BEST | Rohde et al. (2013) | Interpolation | 1° | temp. | Berkeley Earth |
| UDEL | Matsuura and Willmott (2007) | Interpolation | 0.5° | precip. | University of Delaware |

[*] In units of deaths per 100,000 population.
[†] To remove outliers, particularly in low-population regions, we winsorize the mortality rate at the 1% level at high end of the distribution across administrative regions, separately for each country.
[□] All covariate values shown are averages over the years in each country sample.
[×] ADM2 refers to the second administrative level (e.g., county), while ADM1 refers to the first administrative level (e.g., state). NUTS2 refers to the Nomenclature of Territorial Units for Statistics $2^{nd}$ (NUTS2) level, which is specific to the European Union (EU) and falls between first and second administrative levels.
[◇] Global population share for each country in our sample is shown for the year 2010.
[⊗] GDP per capita values shown are in constant 2005 dollars purchasing power parity (PPP).
[⊘] Average daily temperature and annual average of the number of days above 28°C are both population weighted, using population values from 2010.
[‡] EU data for 33 countries were obtained from a single source. Detailed description of the countries within this region is presented in Appendix B.1.
[▷] Most countries in the EU data have records beginning in the year 1990, but start dates vary for a small subset of countries. See Appendix B.1 and Table B1 for details.
[⊕] We separate France from the rest of the EU, as higher resolution mortality data are publicly available for France.
[^] It is widely believed that data from India understate mortality rates due to incomplete registration of deaths.

### 3.1.3 Covariate data

The analysis allows for heterogeneity in the age-specific mortality-temperature relationship as a function of two long-run covariates: a measure of climate (in our main specification, long-run average temperature) and income per capita. We assemble time-invariant measures of both these variables at the ADM1 unit (e.g., state) level using GMFD climate data and a combination of the Penn World Tables (PWT), Gennaioli et al. (2014), and Eurostat (2013). These covariates are measured at ADM1 scale (as opposed to the ADM2 scale of the mortality records) due to limited availability of higher resolution income data. The construction of the income variable requires some estimation to downscale to ADM1 level; details on this procedure are provided in Appendix B.3.

In a set of robustness checks detailed in Section 4.2 and Appendix D.6, we analyze five additional sources of heterogeneity, each of which has been suggested in the literature as an important driver of long-run wellbeing (Alesina and Rodrik, 1994; Glaeser et al., 2004; La Porta and Shleifer, 2014; Bailey and Goodman-Bacon, 2015; World Bank, 2020). These data include country-by-year obvservations of institutional quality

from the Center for Systemic Peace (2020), access to healthcare services and labor force informality from the World Bank (2020), educational attainment from the World Bank (2020) and Organization of Economic Cooperaton and Development (2020), and within-country income inequality from the World Inequality Lab (2020).

## 3.2 Data for projecting the mortality-temperature relationship around the world & into the future

### 3.2.1 Unit of analysis for projections

We partition the global land surface into a set of 24,378 regions and for each region we generate location-specific projected damages of climate change. The finest level of disaggregation in previous estimates of global climate change damages divides the world into 170 regions (Burke, Hsiang, and Miguel, 2015), but most papers account for much less heterogeneity (Nordhaus and Yang, 1996; Tol, 1997). These regions (hereafter, *impact regions*) are constructed such that they are either identical to, or are a union of, existing administrative regions. They (i) respect national borders, (ii) are roughly equal in population across regions, and (iii) display approximately homogenous within-region climatic conditions. Appendix C details the algorithm used to create impact regions.

### 3.2.2 Climate projections

We use a set of 21 high-resolution, bias-corrected, global climate projections produced by NASA Earth Exchange (NEX) (Thrasher et al., 2012)[6] that provide daily temperature and precipitation through the year 2100. We obtain climate projections based on two standardized emissions scenarios: Representative Concentration Pathways 4.5 (RCP4.5, an emissions stabilization scenario) and 8.5 (RCP8.5, a scenario with intensive growth in fossil fuel emissions) (Van Vuuren et al., 2011; Thomson et al., 2011)).

These 21 climate models systematically underestimate tail risks of future climate change (Tebaldi and Knutti, 2007; Rasmussen, Meinshausen, and Kopp, 2016).[7] To correct for this, we follow Hsiang et al. (2017) by assigning probabilistic weights to climate projections and use 12 surrogate models that describe local climate outcomes in the tails of the climate sensitivity distribution (Rasmussen, Meinshausen, and Kopp, 2016). Figure B2 shows the resulting weighted climate model distribution. The 21 models and 12 surrogate models are treated identically in our calculations and we describe them collectively as the surrogate/model mixed ensemble (SMME). Gridded output from these 33 projections are aggregated to impact regions; full details on the climate projection data are in Appendix B.2.

Only 6 of the 21 models we use to construct the SMME provide climate projections after 2100 for both high and moderate emissions scenarios, and none simulate the impact of a marginal ton of $CO_2$.

[6]The dataset we use, called the NEX-GDDP, downscales global climate model (GCM) output from the Coupled Model Intercomparison Project Phase 5 (CMIP5) archive (Taylor, Stouffer, and Meehl, 2012), an ensemble of models typically used in national and international climate assessments.

[7]The underestimation of tail risks in the 21-model ensemble is for several reasons, including that these models form an ensemble of opportunity and are not designed to sample from a full distribution, they exhibit idiosyncratic biases, and have narrow tails. We are correcting for their bias and narrowness with respect to global mean surface temperature (GMST) projections, but our method does not correct for all biases.

Therefore, to include post-2100 years in our estimates of the mortality partial SCC, we rely on the Finite Amplitude Impulse Response (FAIR) simple climate model, which has been developed especially for this type of calculation (Millar et al., 2017).[8] Details on our implementation of FAIR are in Appendix G.

#### 3.2.3 Socioeconomic projections

Projections of population and income are a critical ingredient in the analysis, and for these we rely on the Shared Socioeconomic Pathways (SSPs), which describe a set of plausible scenarios of socioeconomic development over the $21^{st}$ century. We use SSP2, SSP3, and SSP4, which yield emissions in the absence of mitigation policy that fall between RCP4.5 and RCP8.5 in integrated assessment modeling exercises (Riahi et al., 2017). For population, we use the International Institute for Applied Systems Analysis (IIASA) SSP population projections, which provide estimates of population by age cohort at country-level in five-year increments (IIASA Energy Program, 2016). National population projections are allocated to impact regions based on current satellite-based within-country population distributions from Bright et al. (2012) (see Appendix B.3.3). Projections of national income per capita are similarly derived from the SSP scenarios, using both the IIASA projections and the Organization for Economic Co-operation and Development (OECD) Env-Growth model (Dellink et al., 2015) projections. We allocate national income per capita to impact regions using current nighttime light satellite imagery from the NOAA Defense Meteorological Satellite Program (DSMP). Appendix B.3.2 provides details on this calculation.

Because SSP projections are not available after the year 2100, our calculation of the mortality partial SCC relies on an extrapolation of the relationship between climate change damages and global temperature change to later years; see Section 7 for details.

# 4 Empirical estimates of the mortality-temperature relationship, accounting for income and climate heterogeneity

Here we describe an empirical approach to quantify the heterogeneous impact of temperature on mortality across the globe using historical data. This method allows us to capture differences in temperature sensitivity across distinct populations in our sample, and thus to quantify the benefits of adaptation as observed historically. The following section details how we combine this empirical information with standard projection data to construct estimates of the mortality risk of climate change, accounting for the benefits of adaptation.

## 4.1 Empirical model

We estimate the mortality-temperature relationship using a pooled sample of age-specific mortality rates across 40 countries. The effect of temperature on mortality rates is identified using year-to-year variation in the distribution of daily weather following, for example, Deschênes and Greenstone (2011). Additionally,

[8] FAIR is a zero-dimensional structural representation of the global climate designed to capture the temporal dynamics and equilibrium response of global mean surface temperature to greenhouse gas forcing. Appendix G shows that our simulation runs with FAIR create warming distributions that match those from the climate projections in the high-resolution models in the SMME.

we allow the effect of temperature to vary with average temperature (i.e., long-run climate) and average per capita incomes.[9] This approach provides separate estimates for the effect of climate-driven adaptation and income growth on the shape of the mortality-temperature relationship, as they are observed in the historical record.

The two factors defining this interaction model reflect the economics governing adaptation. First, a higher long-run average temperature incentivizes investment in heat-related adaptive behaviors, as the return to any given adaptive mechanism is higher the more frequently the population experiences days with life-threatening temperatures. Second, higher incomes relax agents' budget constraints and hence facilitate adaptive behavior. In other words, people live successfully in both Anchorage, AK and Houston, TX due to compensatory responses to their climate, while the wealthy purchase more safety. To capture these effects, we interact a nonlinear temperature response function with location-specific measures of climate and per capita income.

We fit the following model:

$$M_{ait} = g_a(\boldsymbol{T}_{it}\ ,\ TMEAN_s, \log(GDPpc)_s) + q_{ca}(\boldsymbol{R}_{it}) + \alpha_{ai} + \delta_{act} + \varepsilon_{ait}, \tag{5}$$

where $a$ indicates age category with $a \in \{< 5, 5\text{-}64, > 64\}$, $i$ denotes the second administrative level (ADM2, e.g., county),[10] $s$ refers to the first administrative level (ADM1. e.g., state or province), $c$ denotes country, and $t$ indicates years. Thus, $M_{ait}$ is the age-specific all-cause mortality rate in ADM2 unit $i$ in year $t$. $\alpha_{ai}$ is a fixed effect for $age \times ADM2$, and $\delta_{act}$ a vector of fixed effects that allow for shocks to mortality that vary at the $age \times country \times year$ level.

Our focus in Equation 5 is the effect of temperature on mortality, conditional on average climate and income, which is represented by the age-specific response function $g_a(\cdot)$. Before describing the functional form of this response, we note that our climate data are provided at the grid-cell-by-day level. To align gridded daily temperatures with annual administrative mortality records, we first take nonlinear functions of grid-level daily average temperature and sum these values across the year. We then collapse annual observations across grid cells within each ADM2 using population weights in order to represent temperature exposure for the average person within an administrative unit.[11] This process allows for the recovery of a nonlinear relationship between mortality and temperature at the grid cell level, even though Equation 5 is estimated at a higher level of aggregation (Hsiang, 2016). The nonlinear transformations of daily temperature

[9] These two factors have been the focus of studies modeling heterogeneity across the broader climate-economy literature. For examples, see Mendelsohn, Nordhaus, and Shaw (1994); Kahn (2005); Auffhammer and Aroonruengsawat (2011); Hsiang, Meng, and Cane (2011); Graff Zivin and Neidell (2014); Moore and Lobell (2014); Davis and Gertler (2015); Heutel, Miller, and Molitor (2017); Isen, Rossin-Slater, and Walker (2017).

[10] This is usually the case. However, as shown in Table 1, the EU data is reported at Nomenclature of Territorial Units for Statistics $2^{nd}$ (NUTS2) level, and Japan reports mortality at the first administrative level.

[11] Specifically, we summarize gridded daily average temperatures $T_{zd}$ across grid cells $z$ and days $d$ to create the annual ADM2-level vector $\boldsymbol{T}_{it}$ as follows:

$$\boldsymbol{T}_{it} = \left[ \sum_{z \in i} w_{zi} \sum_{d \in t} T_{zd}, \sum_{z \in i} w_{zi} \sum_{d \in t} T_{zd}^2, \sum_{z \in i} w_{zi} \sum_{d \in t} T_{zd}^3, \sum_{z \in i} w_{zi} \sum_{d \in t} T_{zd}^4 \right]$$

Aggregation across grid cells within an ADM2 is conducted using time-invariant population weights $w_{zi}$, which represent the share of $i$'s population that falls into grid cell $z$ (see Appendix B.2.4 for details).

are captured by the annual, ADM2-level vector $\boldsymbol{T}_{it}$, and we then choose $g_a(\cdot)$ to be a *linear* function of the *nonlinear* elements of $\boldsymbol{T}_{it}$.

In our main specification, $\boldsymbol{T}_{it}$ contains fourth order polynomials of daily average temperatures, summed across the year. We emphasize results from the polynomial model because it strikes a balance between providing sufficient flexibility to capture important nonlinearities, parsimony, and limiting demands on the data. Analogous to temperature, we summarize daily grid-level precipitation in the annual ADM2-level vector $\boldsymbol{R}_{it}$. We construct $\boldsymbol{R}_{it}$ as a second-order polynomial of daily precipitation, summed across the year, and estimate an age- and country-specific linear function of this vector, represented by $q_{ac}(\cdot)$.

In a set of robustness checks we explore the sensitivity of the results to alternative functional forms for temperature. Specifically, we alternatively define $\boldsymbol{T}_{it}$ as a vector of binned daily average temperatures, as a vector of restricted cubic splines of daily average temperatures, and as a 2-part linear spline of daily average temperatures.[12]

The impact of weather realizations $\boldsymbol{T}_{it}$ on mortality is identified from the plausibly random year-to-year variation in temperature within a geographic unit. Specifically, the $age \times ADM2$ fixed effects $\alpha_{ai}$ ensure that we isolate within-location year-to-year variation in temperature and rainfall exposure, which is as good as randomly assigned. The $age \times country \times year$ fixed effects $\delta_{act}$ account for any time-varying trends or shocks to age-specific mortality rates which are unrelated to the climate. We explore robustness to alternative sets of fixed effects in Table D2.

The mortality-temperature response function $g_a(\cdot)$ depends on $TMEAN$, the sample-period average annual temperature, and the logarithm of $GDPpc$, the sample-period average of annual GDP per capita. The model does not include uninteracted terms for $TMEAN$ and $GDPpc$ because they are collinear with $\alpha_{ai}$, which effectively shuts down the possibility of the climate influencing the mortality rate equally on all days, regardless of daily temperature. This is because we define climate adaptation to be actions or investments that reduce the risk of temperatures that threaten human well-being, as is common in the literature (e.g., Hsiang (2016)). The paper's analysis therefore allows the benefits (and, as discussed later, the costs) of adaptation to influence the shape of the mortality-temperature relationship, but not its level.

We implement a form of $g_a(\cdot)$ that exploits linear interactions between the ADM1-level covariates and all nonlinear elements of the temperature vector $\boldsymbol{T}_{it}$. While long-run climate and GDP per capita enter linearly, they are interacted with all the terms of the fourth order polynomial $\boldsymbol{T}_{it}$. More details on implementation of this regression are given in Appendix D.1.[13] We estimate Equation 5 without any regression weights since

[12] In the binned specification, annual values are calculated as the number of days in region $i$ in year $t$ that have an average temperature that falls within a fixed set of 5°C bins. The bin edges are positioned at the locations $\{-\infty, -15, -10, -5, 0, 5, 10, 15, 20, 25, 30, 35, +\infty\}$ in °C. In the restricted cubic spline specification, daily spline terms are summed across the year and knots are positioned at the locations $\{-12, -7, 0, 10, 18, 23, 28, 33\}$ in °C. In the linear spline specification, heating degree days below 0°C and cooling degree days above 25°C are summed across the year.

[13] To see how we implement Equation 5 in practice, let $\boldsymbol{\beta}_a$ indicate the vector of four coefficients that describes the age-specific fourth-order polynomial mortality-temperature response function. In estimating Equation 5, we allow $\boldsymbol{\beta}_a$ to change with climate and income by modeling each element of $\boldsymbol{\beta}_a$ as a linear function of these two variables. Using this notation, our estimating equation is:

$$M_{ait} = \underbrace{(\boldsymbol{\gamma}_{0,a} + \boldsymbol{\gamma}_{1,a} TMEAN_s + \boldsymbol{\gamma}_{2,a} \log(GDPpc)_s)}_{\boldsymbol{\beta}_a} \boldsymbol{T}_{it} + q_{ca}(\boldsymbol{R}_{it}) + \alpha_{ai} + \delta_{act} + \varepsilon_{ait},$$

where $\boldsymbol{\gamma}_{0,a}, \boldsymbol{\gamma}_{1,a}$, and $\boldsymbol{\gamma}_{2,a}$ are each vectors of length four, the latter two describing the effects of $TMEAN$ and $\log(GDPpc)$ on the sensitivity of mortality $M_{ait}$ to temperature $\boldsymbol{T}_{it}$.

we are explicitly modeling heterogeneity in treatment effects rather than integrating over it (Solon, Haider, and Wooldridge, 2015).

A central challenge in understanding the extent of adaptation is that there exists no experimental or quasi-experimental variation in *climate* as opposed to *weather*. Put simply, meaningful variation in climate within a location is not available in recorded history. So, while plausibly random year-to-year fluctuations in temperature within locations are used to identify the effect of weather events in Equation 5, we must use *cross-sectional variation* in climate and income between locations to estimate heterogeneity in the mortality-temperature relationship. We therefore interpret our heterogeneity results as associational.

Nevertheless, we believe this model generates informative estimates of the impact of climate change on mortality for several reasons, including: alternative sources of heterogeneity in mortality sensitivity to temperature have little effect on the estimated response functions; the model performs well out-of-sample on a variety of cross-validation tests; and estimated response functions are robust to a host of alternative specifications. These tests are discussed in detail in Section 4.2.

## 4.2 Empirical results

Tabular results for the estimation of Equation 5 are reported in Table D1 for each of the three age groups. As these terms are difficult to interpret, we visualize this heterogeneity by dividing the sample into terciles of income and terciles of climate (i.e., the two interaction terms), and then further dividing the sample into the intersection of these two groups of three. This partitions the $\log(GDPpc) \times TMEAN$ space into nine subsamples. We plot predicted response functions at the mean value of climate and income within each of these nine subsamples, using the coefficients in Table D1. The result is a set of predicted response functions that vary across the joint distribution of income and average temperature within the sample data. The resulting response functions are shown in Figure 1 for the >64 age category (other age groups are shown in Appendix D.1), where average incomes are increasing across subsamples vertically and average temperatures are increasing across subsamples horizontally.

The Figure 1 results are broadly consistent with the economic prediction that people adapt to their climate and that income is protective. For example, within each income tercile in Figure 1, the effect of hot days (e.g., days >35°C) declines as one moves from left (cold climates) to right (hot climates). This finding reflects that individuals and societies make compensatory adaptations in response to their climate (e.g., people install air conditioning in hot climates more frequently than in cold ones). With respect to income, Figure 1 reveals that moving from the bottom (low income) to top (high income) within a climate tercile causes a substantial flattening of the response function, especially at high temperatures. Thus, protection from extreme temperatures appears to be a normal good.

Two statistics help to summarize the findings from Figure 1. First, in the >64 age category across all income values, moving from the coldest to the hottest tercile saves on average 7.9 ($p$-value=0.06) deaths per 100,000 at 35°C. Second, moving from the poorest to the richest tercile across all climate values in the sample saves approximately 5.0 ($p$-value=0.1) deaths per 100,000 at 35°C for the > 64 age category.

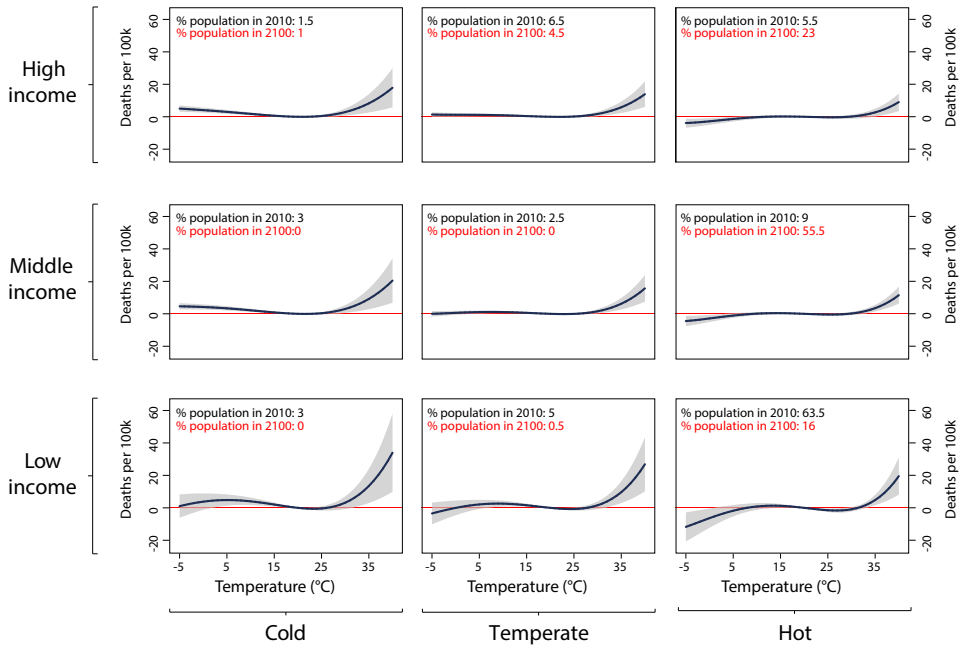


**Figure 1: Heterogeneity in the mortality-temperature relationship (age >64 mortality rate).** Each panel represents a predicted mortality-temperature response function for the >64 age group for a subset of the income-average temperature covariate space within our data sample. Response functions in the lower left apply to the low-income, cold regions of our sample, while those in the upper right apply to the high-income, hot regions of our sample. Regression estimates are from a fourth-order polynomial in daily average temperature and are estimated using GMFD weather data with a sample that was winsorized at the 1% level on the top end of the distribution only. All response functions are estimated jointly in a stacked regression model that is fully saturated with age-specific fixed effects, and where each temperature variable is interacted with each covariate. Values in the top left-hand corner of each panel show the percentage of the global population that reside within each in-sample tercile of average income and average temperature in 2010 (black text) and as projected in 2100 (red text, SSP3). Other age groups are shown in Figures D1 and D2.

## 4.3 Sensitivity analyses

### 4.3.1 Age group heterogeneity

Consistent with prior literature (e.g., Deschênes and Moretti, 2009; Heutel, Miller, and Molitor, 2017), we uncover substantial heterogeneity across age groups within our multi-country sample. Figure 2 displays the average mortality-temperature response for each of our three age categories (<5, 5-64, >64),[14] while Appendix D.1 shows the influence of income and climate on the mortality-temperature relationships for each age group. On average across the globe, we find that people over the age of 64 experience approximately 4.7 extra deaths per 100,000 for a day at 35°C (95°F) compared to a day at 20°C (68°F), a substantially larger effect than that for younger cohorts, which exhibit little response. This age group is also more severely affected by cold days; estimates suggest that people over the age of 64 experience 3.4 deaths per 100,000 for a day at −5°C (23°F) compared to a day at 20°C, while there is a relatively weak mortality response to these cold days for other age categories. Overall, these results demonstrate that the elderly are disproportionately harmed by additional hot days and disproportionately benefit from reductions in cold days.

[14] Age-specific regression estimates in Figure 2 are estimated jointly in a stacked regression model that is fully saturated with age-specific fixed effects and has no income or climate interaction terms (Equation D.17). See Appendix D.2.1 for details.

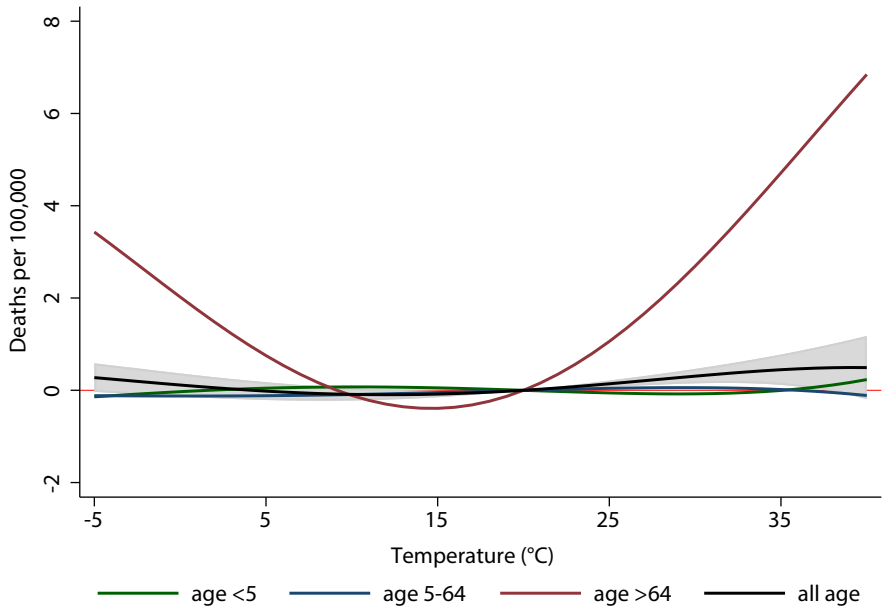


**Figure 2: Mortality-temperature response function with demographic heterogeneity.** Mortality-temperature response functions are estimated for populations <5 years of age (green), between 5 and 64 years of age (blue), >64 years of age (red), and pooled across all ages (black, with associated 95% confidence intervals shaded in grey). Regression estimates shown are from a fourth-order polynomial in daily average temperature and are estimated using GMFD weather data with a sample that was winsorized at the 1% level. All age-specific response functions are estimated jointly in a stacked regression model that is fully saturated with age-specific fixed effects (Equation D.17). Confidence intervals are shown only for the all-age response function; statistical significance for age-specific response functions can be seen in Table D2.

#### 4.3.2 Alternative fixed effects

Table D2 reports on the robustness of the estimated mortality-temperature relationship to alternative spatial and temporal controls. Tabular results show the average multi-country marginal effect of temperature evaluated at various temperatures. These estimates can be interpreted as the change in the number of deaths per 100,000 per year resulting from one additional day at each temperature, compared to the reference day of 20°C (68°F). Columns (1)-(3) increase the saturation of temporal controls in the model specification, ranging from country-year fixed effects in column (1) to country-year-age fixed effects in column (2), and adding age-specific state-level linear trends in column (3). Our preferred specification is column (2), as column (1) does not account for differential temporal shocks to mortality rates by age group, while in column (3) we cannot reject the null of equal age-specific, ADM1-level trends. However, estimated age-specific responses are similar across all specifications. This result is robust to alternative functional form assumptions (i.e., different nonlinear functions of $\boldsymbol{T}_{it}$), including a non-parametric binned regression, as well as to the use of alternative, independently-sourced, climate datasets (Figure D3).

#### 4.3.3 Alternative specifications

In Table D2, columns (4) and (5) provide results for the average mortality-temperature relationship under alternative specifications. In column (4), we address the fact that some of the data are drawn from countries which may have less capacity for data collection than others in the sample. Because the mortality data are collected by institutions in different countries, it is possible that some sources are systematically less precise. To account for this, we re-estimate the model using Feasible Generalized Least Squares (FGLS) under the assumption of constant variance within each ADM1 unit.[15] In column (5), we allow for the possibility that temperatures can exhibit lagged effects on health and mortality (e.g., Deschênes and Moretti, 2009; Barreca et al., 2016; Guo et al., 2014). Lagged effects within and across months in the same calendar year are accounted for in the net annual mortality totals used in all specifications. However, it is possible that temperature exposure in December of each year affects mortality in January of the following year. To account for this, in column (5) we define a 13-month exposure window to additionally account for temperatures previous December.[16] Table D2 shows that the results for both of these alternative specifications are similar in sign and magnitude to those from column (2).

Figure D3 displays the results of estimating the mortality-temperature relationship using a set of alternative functional forms of temperature (i.e., different formulations of the temperature vector $\boldsymbol{T}_{it}$) and using two different climate datasets to obtain those temperatures (see Appendix B.2 for details on these climate datasets). We explore three functional forms in addition to the main fourth-order polynomial specification: bins of daily average temperature, restricted cubic splines, and piecewise linear splines. The first two are especially demanding of the data, particularly in the context of Equation 5, which allows for heterogeneity in temperature sensitivity. Overall, the results for these alternative functional form specifications are similar to the fourth-order polynomial when using both climate datasets (see Appendix D.2 for details).

Finally, we find that the coefficients in Equation 5 are qualitatively unchanged when we use alternative characterizations of the climate (see Appendix D.4) or if we omit precipitation controls (see Appendix D.5).

#### 4.3.4 Additional sources of heterogeneity

In order to predict responses around the world and inform projections of damages in the future, it is necessary for all covariates in Equation 5 to be available globally today, at high spatial resolution, *and* that credible projections of their future evolution are available. One reason we use average incomes and climate in Equation 5 is that both variables meet these criteria.

However, a valid critique of this model is that other factors likely explain heterogeneity in the mortality-temperature relationship, yet are omitted from Equation 5. To address this possibility, we collect data on five other candidate variables that could explain heterogeneity in mortality sensitivity to temperature, such

[15] To do this, we estimate the model in Equation D.17 using population weights and our preferred specification (column (2)). Using the residuals from this regression, we calculate an ADM1-level weight that is equal to the average value of the squared residuals, where averages are taken across all ADM2-age-year level observations that fall within a given ADM1. We then inverse-weight the regression in a second stage, using this weight. All ADM2-age-year observations within a given ADM1 are assigned the same weight in the second stage, where ADM1 locations with lower residual variance are given higher weight. For some ADM2s, there are insufficient observations to identify age-specific variances; to ensure stability, we dropped the ADM2s with less than 5 observations per age group. This leads us to drop 246 (of >800,000) observations in this specification.

[16] The specification in column (5) defines the 13-month exposure window such that for a given year $t$, exposure is calculated as January to December temperatures in year $t$ *and* December temperature in year $t-1$.

as institutional quality, doctors per capita, and educational attainment.[17] Appendix D.6 shows that adding these variables as additional interaction terms when estimating Equation 5 generates very similar predicted response functions in historical data. This suggests that a model which employs only income and climate explains a large amount of the heterogeneity across space.

Further, we find that including only climate and income as interaction effects out-performs a model that includes additional interaction terms when those variables are not available in future projections. Appendix D.6 shows that including these potential determinants of heterogeneity when estimating Equation 5, but omitting them when generating predictions (as would be necessary when making climate change impact projections), substantially increases prediction error.

#### 4.3.5 Out-of-sample performance

In the next section, we use coefficients estimated from Equation 5, in combination with local-level observations and projections of $TMEAN$ and $\log(GDPpc)$, to generate predicted response functions in all regions of the world, including where mortality data are unavailable, both in the present and into future. To assess the performance of our model in predicting mortality-temperature relationships out-of-sample, we implement multiple custom cross-validation exercises designed to mimic the spatial and temporal extrapolation that is required when using available historical data to generate global climate change projections decades into the future. These tests are described in detail in Appendix D.7, but we summarize their results here.

We perform three cross-validation exercises. In each case, we compare the performance of Equation 5 to the performance of a benchmark model without $TMEAN$ and $\log(GDPpc)$ interactions; that is, a model that ignores adaptation and benefits of income. We do so because most prior literature has estimated impacts of climate change using spatially and/or temporally homogeneous response functions (e.g., Hsiang et al., 2017; Deschênes and Greenstone, 2011). The first exercise uses standard $k$-fold cross-validation (Friedman et al., 2001), but constrains all observations within an ADM1 (e.g., state) to remain in either the "testing" or the "training" sample within each fold, in order to account for spatial and temporal correlation within these regions. The second exercise subsamples the data based on the in-sample distributions of $TMEAN$ and $\log(GDPpc)$ and tests the model's ability to predict mortality rates in populations with different incomes and climates than the estimation sample. The final exercise subsamples data based on time, testing the model's ability to predict future mortality-temperature relationships.

In all three cases, we find that the model in Equation 5 performs well, both when compared to measures of in-sample model fit and when compared to the out-of-sample performance of a model that omits interaction effects. In particular, Equation 5 performs well in predicting mortality rates in the lowest income and hottest locations, even when those locations are omitted from the estimating sample (see Panel B of Table D5). This is an important result, given the under-representation of low income and hot climates in our mortality records, relative to the global population (see Figure 3). We investigate this finding further in Appendix D.8, where we show strong predictive performance in India, a hot and relatively poor country that is not used in estimation due to its lack of age-specific mortality rates. We do find that Equation 5

[17] In collecting these data, we note that obtaining any of them at subnational scales is a substantial challenge and in most cases not possible. See Appendix D.6 for details.

occasionally over-estimates or under-estimates future mortality sensitivity to hot days in some age groups and for some income levels (see Figure D9). To address this concern, we explore in Appendix F.4 the sensitivity of our main climate change projections to alternative assumptions about the rates of adaptation.

# 5 Projections of climate change impacts on future mortality rates

This section begins by using the empirical results from Section 4 to extrapolate mortality-temperature relationships to the parts of the world where historical mortality data are unavailable. We then combine these estimates with projected changes in climate exposure and income growth to quantify expected climate change induced mortality risk, accounting for climate model and econometric uncertainty. The paper's ultimate aim is to develop an estimate of the full mortality-related costs of climate change (i.e., the sum of the increase in deaths and adaptation costs shown in Equation 4), but adaptation costs are not observed directly (see Section 2). Therefore, here we display empirically-derived estimates of changes in mortality rates due to climate change, highlighting the difference between projections that do and do not account for the benefits of adaptation. In the following section, we use a stylized revealed preference approach to infer adaptation costs, which allows for a complete measure.

## 5.1 Defining three measures of climate change impacts

Here we define three measures of climate change impacts that elucidate the roles of adaptation and income growth in determining the full mortality-related costs of climate change. The empirical estimation of each of these measures is first reported in units of deaths per 100,000 using the estimates of $\hat{g}_a(\cdot)$ reported in Section 4, although it is straightforward to monetize these measures using estimates of the value of a statistical life (VSL), and we do so in the next section.

The first measure is the *mortality effects of climate change with neither adaptation nor income growth*, which provides an estimate of the increases in mortality rates when each impact region's response function in each year $t$ is a function of their initial period (indicated as $t_0$) level of income and average climate (recall Equation 2). In other words, mortality sensitivity to temperature is assumed not to change with future income or temperature. This is a benchmark model often employed in previous work. Specifically, the expected climate induced mortality risk that we estimate for an impact region and age group in a future year $t$ under this measure are (omitting subscripts for impact regions and age groups for clarity):[18]

(i) *Mortality effects of climate change with neither adaptation nor income growth*:

$$\underbrace{\hat{g}(\boldsymbol{T}_t, TMEAN_{t_0}, \log(GDPpc)_{t_0})}_{\substack{\text{mortality risk with climate change} \\ \text{and without adaptation}}} - \underbrace{\hat{g}(\boldsymbol{T}_{t_0}, TMEAN_{t_0}, \log(GDPpc)_{t_0})}_{\text{current mortality risk}}$$

The second measure is the *mortality effects of climate change with benefits of income growth*, which allows response functions to change with future incomes. This measure captures the change in mortality rates that

[18]Note that in all estimates of climate change impacts, population growth is accounted for as an exogenous projection that does not depend on the climate.

would be expected from climate change if populations became richer, but they did not respond optimally to warming by adapting above and beyond how they would otherwise cope with their historical climate. This measure is defined as:

(ii) *Mortality effects of climate change with benefits of income growth*:

$$\underbrace{\hat{g}(\boldsymbol{T}_t, TMEAN_{t_0}, \log(GDPpc)_t)}_{\substack{\text{mortality risk with climate change} \\ \text{and benefits of income growth}}} - \underbrace{\hat{g}(\boldsymbol{T}_{t_0}, TMEAN_{t_0}, \log(GDPpc)_t)}_{\substack{\text{mortality risk without climate change} \\ \text{and with benefits of income growth}}}$$

Note that in expression (ii), the second term represents a counterfactual predicted mortality rate that would be realized under current temperatures, but in a population that benefits from rising incomes over the coming century. This counterfactual includes the prediction, for example, that air conditioning will become much more prevalent in a country like India as the economy grows, regardless of whether climate change unfolds or not.

The third measure is the *mortality effects of climate change with benefits of income growth and adaptation*, and in this case populations adjust to experienced temperatures in the warming scenario (recall Equation 3). This metric is an estimate of the observable deaths that would be expected under a warming climate, accounting for the benefits of optimal adaptation and income growth:

(iii) *Mortality effects of climate change with benefits of income growth and adaptation*:

$$\underbrace{\hat{g}(\boldsymbol{T}_t, TMEAN_t, \log(GDPpc)_t)}_{\substack{\text{mortality risk with climate change, benefits} \\ \text{of income growth, and adaptation}}} - \underbrace{\hat{g}(\boldsymbol{T}_{t_0}, TMEAN_{t_0}, \log(GDPpc)_t)}_{\substack{\text{mortality risk without climate change} \\ \text{and with benefits of income growth}}}$$

As above, expression (iii) includes the subtraction of a counterfactual in which incomes rise but climate is held fixed.

Year $t_0$ is treated as the baseline period, which we define to be the years 2001-2010, so we are measuring the impact of climate change since this period.[19] These three measures are all reported below in units of deaths per 100,000, using the estimates of $\hat{g}(\cdot)$ shown in Section 4.

## 5.2 Methods for climate change projection: spatial extrapolation

The fact that carbon emissions are a global pollutant requires that estimates of climate damages used to inform an SCC must be global in scope. A key challenge for generating such globally-comprehensive estimates in the case of mortality is the absence of data throughout many parts of the world. Often, registration of births and deaths does not occur systematically. Although we have, to the best of our knowledge, compiled the most comprehensive mortality data file ever collected, our 40 countries only account for 38% of the global population (55% if India is included, although it only contains all-age mortality rates). This leaves more than 4.2 billion people unrepresented in the sample of available data, which is especially troubling because

[19] While anthropogenic warming has been detected in the climate record far earlier than 2001-2010, we estimate impacts of climate change only since this period.

these populations have incomes and live in climates that may differ from the parts of the world where data are available.

To achieve the global coverage essential to understanding the costs of climate change, we use the results from the estimation of Equation 5 on the observed 38% global sample to estimate the sensitivity of mortality to temperature everywhere, including the unobserved 62% of the world's population. Specifically, the results from this model enable us to use two observable characteristics – average temperature and income – to predict the mortality-temperature response function for each of our 24,378 impact regions. Importantly, it is not necessary to recover the overall mortality rate for these purposes.

To see how this is done, we note that the projected response function for any impact region $r$ requires three ingredients. The first are the estimated coefficients $\hat{g}_a(\cdot)$ from Equation 5. The second are estimates of GDP per capita at the impact region level.[20] And third is the average annual temperature (i.e., a measure of the long-run climate) for each impact region, where we use the same temperature data that were assembled for the regression in Equation 5.

We then predict the shape of the response function for each age group $a$, impact region $r$, and year $t$, up to a constant: $\hat{g}_{art} = \hat{g}_a(\boldsymbol{T}_{rt}, TMEAN_{rt}, \log(GDPpc)_{rt})$. The various fixed effects in Equation 5 are unknown and omitted, since they were nuisance parameters in the original regression. This results in a unique, spatially heterogeneous, and globally comprehensive set of predicted response functions for each location on Earth.

The accuracy of the predicted response functions will depend, in part, on its ability to capture responses in regions where mortality data are unavailable. An imperfect but helpful exercise when considering whether our model is representative is to evaluate the extent of common overlap between the two samples. Figure 3A shows this overlap in 2015, where the grey squares reflect the joint distribution of GDP and climate in the full global partition of 24,378 impact regions and orange squares represent the analogous distribution only for the impact regions in the sample used to estimate Equation 5. It is evident that temperatures in the global sample are generally well-covered by our data, although we lack coverage for the poorer end of the global income distribution due to the absence of mortality data in poorer countries. As discussed in Section 4, we explore this extrapolation to lower incomes with a set of robustness checks in Appendix D.

### 5.3 Methods for climate change projection: temporal extrapolation

As discussed in Section 2, a measure of the full mortality risk of climate change must account for the benefits that populations realize from optimally adapting to a gradually warming climate, as well as from income growth relaxing the budget constraint and enabling compensatory investments. Thus, we allow each impact region's mortality-temperature response function to evolve over time, reflecting projected changes in climate and incomes that come from a set of internationally standardized and widely used scenarios. Specifically, we model the evolution of response functions in region $r$ and year $t$ based on these projections and the estimation results from fitting Equation 5.

Some details about these projections are worth noting. First, a 13-year moving average of income per

[20] The procedure is described in Section 3.2 and Appendix B.3.2

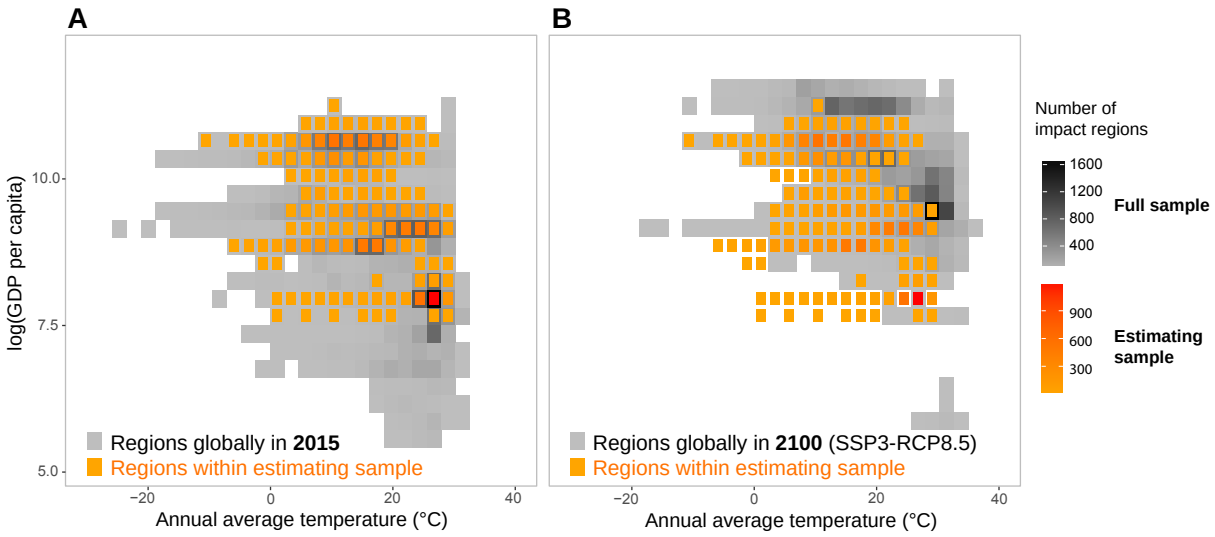


**Figure 3: Joint coverage of income and long-run average temperature for estimating and full samples.** Joint distribution of income and long-run average annual temperature in the estimating sample (red-orange), as compared to the global sample of impact regions (grey-black). Panel A shows in grey-black the global sample for regions in 2015. Panel B shows in grey-black the global sample for regions in 2100 under a high-emissions scenario (RCP8.5) using climate model CCSM4 and a median growth scenario (SSP3). In both panels, the in-sample frequency in red-orange indicates coverage for impact regions within our data sample in 2015.

capita in region $r$ is calculated using national forecasts from the Shared Socioeconomics Pathways (SSP), combined with a within-country allocation of income based on present-day nighttime lights (see Appendix B.3.2), to generate a new value of $\log(GDPpc)_{rt}$. The length of this time window is chosen based on a goodness-of-fit test across alternative window lengths (see Appendix E.1). Second, a 30-year moving average of temperatures for region $r$ is updated in each year $t$ to generate a new level of $TMEAN_{rt}$. Finally, the response curves $\hat{g}_{art} = \hat{g}_a(\boldsymbol{T}_{rt}, TMEAN_{rt}, \log(GDPpc)_{rt})$ are calculated for each region for each age group in each year with these updated values of $TMEAN_{rt}$ and $\log(GDPpc)_{rt}$.

Figure 3B shows that over the coming decades, temperatures and incomes are predicted to rise beyond the support of the global cross-section in our data. Thus, we must impose two constraints, guided by economic theory and by the physiological literature, to ensure that future response functions are consistent with the fundamental characteristics of mortality-temperature responses in the historical record and demonstrate plausible out-of-sample projections.[21] First, we impose the constraint that the response function must be weakly monotonic around an empirically estimated, location-specific, optimal mortality temperature, called the *minimum mortality temperature* (MMT). That is, we assume that temperatures farther from the MMT (either colder or hotter) must be at least as harmful as temperatures closer to the MMT. This assumption is important because Equation 5 uses within-sample variation to parameterize how the U-shaped response function flattens; with extrapolation beyond the support of historically observed income and climate, this behavior could go "beyond flat", such that extremely hot and cold temperature days reduce mortality relative to the MMT (Figure E1). In fact, this is guaranteed to occur mechanically if enough time elapses, because income and climate interact with the response function linearly in Equation 5. However, such behavior is

[21] See Appendix E.2 for details on these assumptions and their implementation.

inconsistent with a large body of epidemiological and econometric literature recovering U-shaped mortality-temperature relationships under many functional form assumptions and in diverse locations (Gasparrini et al., 2015; Burgess et al., 2017; Deschênes and Greenstone, 2011), as well as what we observe in our data. As a measure of its role in our results, the weak monotonicity assumption binds for the >64 age category at 35°C in 9% and 18% of impact regions in 2050 and 2100, respectively.[22,23]

Second, we assume that rising income cannot make individuals worse off, in the sense of increasing the temperature sensitivity of mortality. Because increased income per capita strictly expands the choice set of individuals considering whether to make adaptive investments, it should not increase the effect of temperature on mortality rates. Consistent with this intuition, we find that income is protective against extreme heat for all age groups. However, for some age groups, the estimation of Equation 5 recovers statistically insignificant but positive effects of income on mortality sensitivity to extreme cold (Table D1). Therefore, we constrain the marginal effect of income on temperature sensitivity to be weakly negative in future projections, although we place no restrictions on the cross-sectional effect of income when estimating Equation 5.[24]

With these two constraints, we project annual impacts of climate change separately for each impact region and age group from 2001 to 2100. Specifically, we apply projected changes in the climate to each region's response function, which is evolving as climate and income evolve. The nonlinear transformations of daily average temperature that are used in the function $g_a(\boldsymbol{T}_{rt})$ are computed under both the RCP4.5 and RCP8.5 emissions scenarios for all 33 climate projections in the SMME (as described in Section 3.2). This distribution of climate models captures uncertainties in the climate system through 2100.

## 5.4 Methods for accounting for uncertainty in projected mortality effects of climate change

An important feature of the analysis is to characterize the uncertainty inherent in these projections of the mortality impacts of climate change.[25] As discussed in Section 5.3, we construct estimates of the mortality risk of climate change for each of 33 distinct climate projections in the SMME that together capture the uncertainty in the climate system.[26] Additionally, uncertainty in the estimates of $\hat{g}_a(\cdot)$ is an important second source of uncertainty in our projected impacts that is independent of physical uncertainty.

In order to account for both of these sources of uncertainty, we execute a Monte Carlo simulation following the procedure in Hsiang et al. (2017). First, for each age category, we randomly draw a set of parameters,

[22]The frequency with which the weak monotonicity assumption binds will depend on the climate model and the emissions and socioeconomic trajectories used; reported statistics refer to the CCSM4 model under RCP8.5 with SSP3.

[23]In imposing this constraint, we hold the MMT fixed over time at its baseline level in 2015 (Figure E1D). We do so because the use of spatial and temporal fixed effects in Equation 5 implies that response function levels are not identified; thus, while we allow the *shape* of response functions to evolve over time as incomes and climate change, we must hold fixed their *level* by centering each response function at its time-invariant MMT. Note that these fixed effects are by definition not affected by a changing weather distribution. Thus, their omission does not influence estimates of climate change impacts.

[24]The assumption that rising income cannot increase the temperature sensitivity of mortality binds for the >64 age category under realized temperatures in 30% and 24% of impact region days in 2050 and 2100, respectively.

[25]See Burke et al. (2015) for a discussion of combining physical uncertainty from multiple models in studies of climate change impacts.

[26]Note that while the SMME fully represents the tails of the climate sensitivity distribution as defined by a probabilistic simple climate model (see Appendix B.2.3), there remain important sources of climate uncertainty that are not captured in our projections, due to the limitations of both the simple climate model and the GCMs. These include some climate feedbacks that may amplify the increase of global mean surface temperature, as well as some factors affecting local climate that are poorly simulated by GCMs.

corresponding to the terms composing $\hat{g}_a(\cdot)$, from an empirical multivariate normal distribution characterized by the covariance between all of the parameters from the estimation of Equation 5.[27] Second, using these parameters in combination with location- and time-specific values of income and average climate provided by a given SSP scenario and RCP-specific climate projection from each of the 33 climate projections in the SMME, we construct a predicted response function for each of our 24,378 impact regions. Third, with these response functions in hand, we use daily weather realizations for each impact region from the corresponding simulation to predict an annual mortality impact. Finally, this process is repeated until approximately 1,000 projection estimates are complete for each impact region, age group, and RCP-SSP combination.

With these ∼1,000 response functions, we calculate the mortality effects of climate change (i.e., expressions (i)-(iii) above) for each impact region for each year between 2001 and 2100. The resulting calculation is computationally intensive, requiring ∼94,000 hours of CPU time across all scenarios reported in the main text and Appendix. When reporting projected impacts in any given year, the reports summary statistics (e.g., mean, median) of this entire distribution.

## 5.5 Results: spatial extrapolation of temperature sensitivity

Figure 4 reports on our extrapolation of mortality-temperature response functions to the entire globe for the >64 age category (see Figure D4 for other age groups). In panel A, these predicted mortality-temperature responses are plotted for each impact region for 2001-2010 average values of income and climate and for the impact regions that fall within the countries in our mortality dataset ("in-sample"). Despite a shared overall shape, panel A reveals substantial heterogeneity across regions in this temperature response. Geographic heterogeneity within our sample is shown for hot days in the map in panel C, where colors indicate the marginal effect of a day at 35°C, relative to a day at a location-specific minimum mortality temperature. Grey areas are locations where mortality data are unavailable.

Panels C and D of Figure 4 show analogous plots, but now extrapolated to the entire globe. We can fill in the estimated mortality effect of a 35°C day for regions without mortality data by using 2001-2010 location-specific information on average income and climate. The predicted responses at the global scale imply that a 35°C day increases the average mortality rate across the globe for the oldest age category by 10.1 deaths per 100,000 relative to a location-specific minimum mortality temperature.[28] It is important to note that the effect in locations without mortality data is 11.7 deaths per 100,000, versus 7.8 within the sample of countries for which mortality data are available, largely driven by the fact that our sample represents wealthier locations where temperature responses are more muted.

Overall, there is substantial heterogeneity across the planet. Additionally, it is evident that the effects of temperature on human well-being are quite different in places where we are and are not able to obtain subnational mortality data.

[27] Note that coefficients for all age groups are estimated jointly in Equation 5, such that across-age-group covariances are accounted for in this multivariate distribution.

[28] This average impact of a 35°C is derived by taking the unweighted average level of the mortality-temperature response function evaluated at 35°C across each of 24,378 impact regions globally.

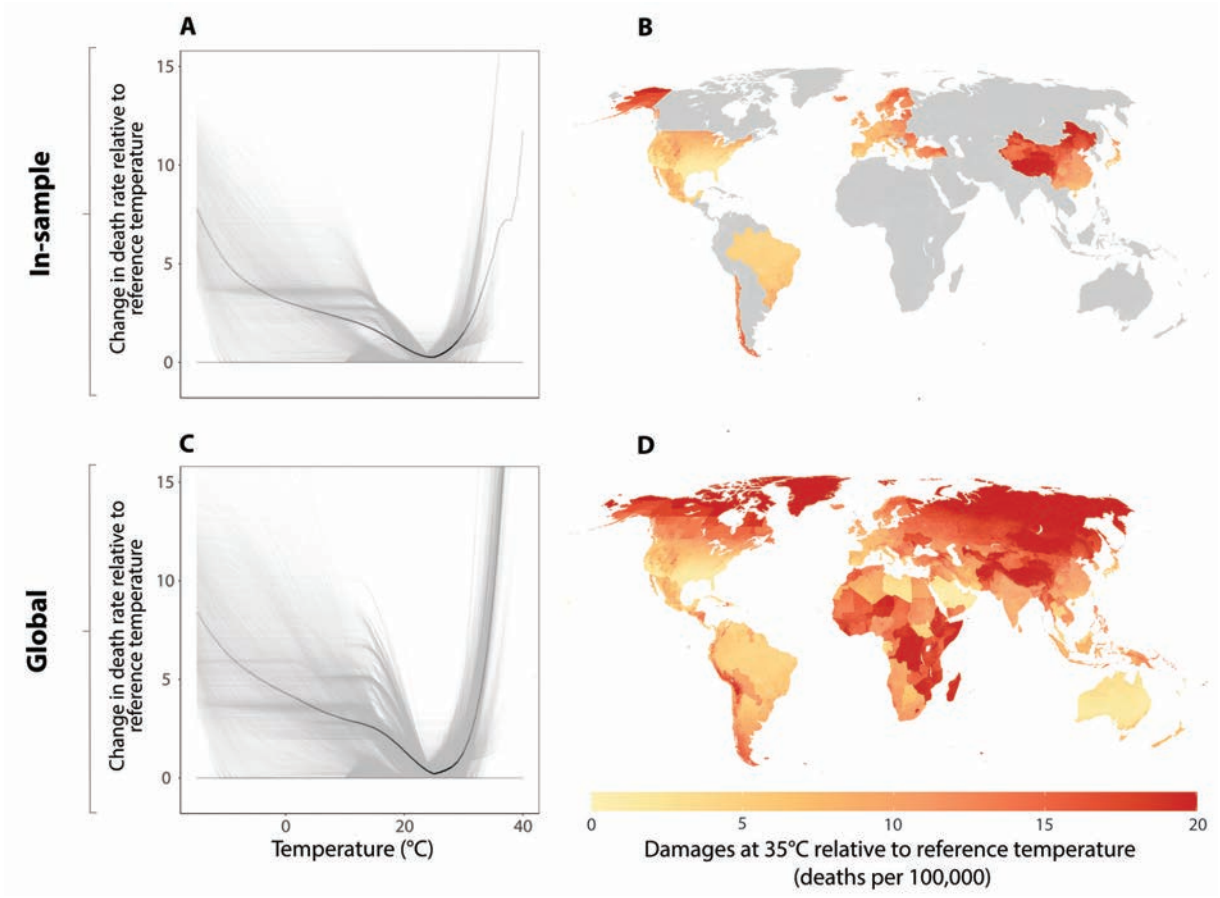


**Figure 4: Using income and climate to predict current response functions globally (age >64 mortality rate).** In panels A and C, grey lines are predicted response functions for impact regions, each representing a population of 276,000 on average. Solid black lines are the unweighted average of the grey lines, where the opacity indicates the density of realized temperatures (Hsiang, 2013). Panels B and D show each impact region's mortality sensitivity to a day at 35°C, relative to a location-specific minimum mortality temperature. The top row shows all impact regions in the sample of locations with historical mortality data (included in main regression tables), and the bottom row shows extrapolation to all impact regions globally. Predictions shown are averages over the period 2001-2010 using the SSP3 socioeconomic scenario and climate model CCSM4 under the RCP8.5 emissions scenario. Figure D4 shows analogous results for other age groups.

## 5.6 Results: projection of future climate change impacts

The previous subsection demonstrated that the model of heterogeneity outlined in Equation 5 allows us to extrapolate mortality-temperature relationships to regions of the world without mortality data today. However, to calculate the full global mortality risks of climate change, it is also necessary to allow these response functions to change through time to capture the benefits of adaptation and the effects of income growth. This subsection reports on using our model of heterogeneity and downscaled projections of income and climate to predict impact region-level response functions for each age group and year, as described in Section 5.3. Uncertainty in these estimated response functions is accounted for through Monte Carlo simulation, as described in Section 5.4. Throughout this subsection, we show results relying on income and population projections from the socioeconomic scenario SSP3 because its historic global growth rates in GDP per capita and population match observed global growth rates over the 2000-2018 period much more closely

than other SSPs (see Table B3). Appendix F shows results using SSP2 and SSP4, and the methodology we develop can be applied to any available socioeconomic scenario.

### 5.6.1 Mortality impacts of climate change for 24,378 global regions

Figure 5 shows the spatial distribution of the mortality effects of climate change with benefits of income growth and adaptation (expression (iii)) in 2100 under the emissions scenario RCP8.5, expressed in death-equivalents per 100,000. Other measures of climate change impacts (expressions (i) and (ii)) are mapped in Appendix Figure F1. To construct these estimates, we generate impact-region specific predictions of mortality damages from climate change for all years between 2001 and 2100, separately for each age group. The map displays the spatial distribution of the mean estimate across our ensemble of Monte Carlo simulations, accounting for both climate and statistical uncertainty and pooling across all age groups.[29] The density plots for select cities show the full distribution of impacts across all Monte Carlo simulations, with the white line equal to the mean estimate displayed on the map.

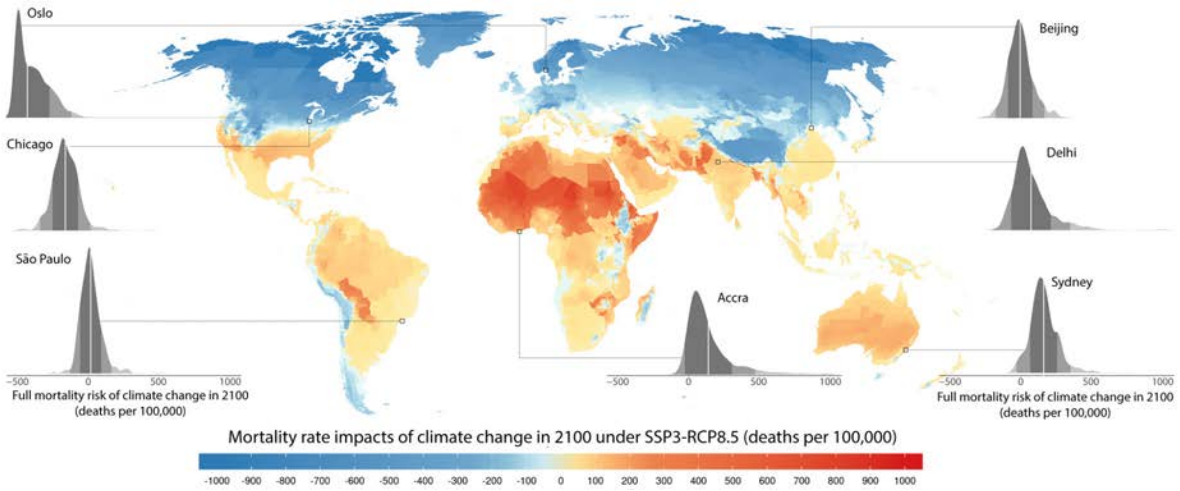


**Figure 5: The mortality impacts of future climate change.** The map indicates the impact of climate change on mortality rates, measured in units of deaths per 100,000 population, in the year 2100. Estimates come from a model accounting for the benefits of adaptation and income growth, and the map shows the climate model weighted mean estimate across Monte Carlo simulations conducted on 33 climate models; density plots for select regions indicate the full distribution of estimated impacts across all Monte Carlo simulations. In each density plot, solid white lines indicate the mean estimate shown on the map, while shading indicates one, two, and three standard deviations from the mean. All values shown refer to the RCP8.5 emissions scenario and the SSP3 socioeconomic scenario. See Figure F6 for an analogous map of impacts for RCP4.5 and SSP3.

Figure 5 makes clear that the costs of climate change-induced mortality risks are distributed unevenly around the world, even when accounting for the benefits of income growth and adaptation. Despite the gains from adaptation shown in Figure E2, there are large increases in mortality risk in the global south. For example, in Accra, Ghana, climate change is predicted to lead to approximately 100 more days >32°C (∼90°F) per year and cause 140 additional deaths per 100,000 annually under RCP8.5 in 2100. If adaptation to climate and benefits of income growth were ignored, climate change would be predicted to cause 260

[29] When calculating mean values across estimates generated for each of the 33 climate models that form our ensemble, we use model-specific weights. These weights are constructed as described in Appendix B.2.3 in order to accurately reflect the full probability distribution of temperature responses to changes in greenhouse gas concentrations.

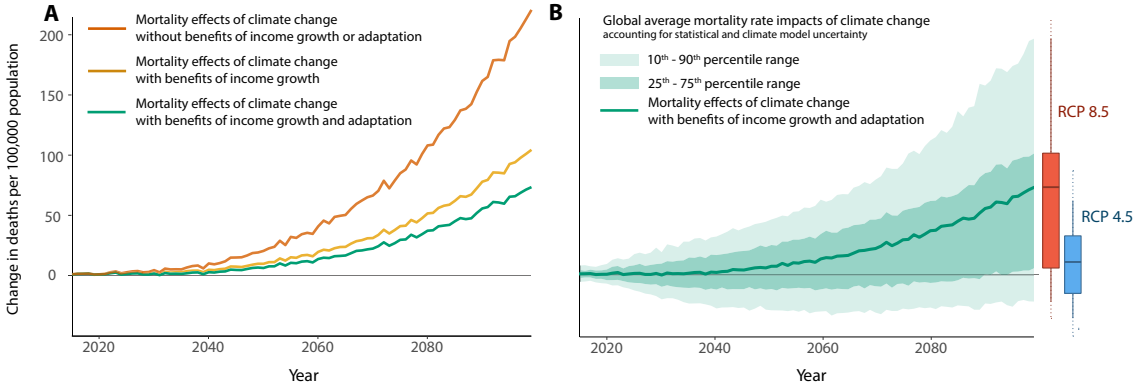


**Figure 6: Time series of projected mortality rate impacts of climate change.** All lines show predicted mortality effects of climate change across all age categories and are represented by a mean estimate across a set of Monte Carlo simulations accounting for both climate model and statistical uncertainty. In panel A, each colored line represents a partial mortality effect. Orange (expression (i)): mortality effects without adaptation. Yellow (expression (ii)): mortality effects with benefits of income growth. Green (expression (iii)): mortality effects with benefits of income growth and adaptation. Panel B shows the $10^{th}$-$90^{th}$ percentile range of the Monte Carlo simulations for the mortality effects with benefits of income growth and adaptation (equivalent to the green line in panel A), as well as the mean and interquartile range. The boxplots show the distribution of mortality rate impacts in 2100 under both RCPs. All line estimates shown refer to the RCP8.5 emissions scenario and all line and boxplot estimates refer to the SSP3 socioeconomic scenario. Figure F7 shows the equivalent for SSP3 and RCP4.5.

additional deaths per 100,000 in this scenario. In contrast, there are gains in many impact regions in the global north, including in London, England, where climate change is predicted to save approximately 70 lives per 100,000 annually. When the benefits of adaptation and income growth are included, these changes amount to a 17% increase in Accra's annual mortality rate and an 8% decline in London's.

### 5.6.2 Aggregate global mortality consequences of climate change

Figure 6 plots predictions of global increases in the mortality rate (deaths per 100,000) for all three measures of climate change impacts, under emissions scenario RCP8.5. The measures are calculated for each of the 24,378 impact regions and then aggregated to the global level. In panel A, each line shows a mean estimate for the corresponding climate change impact measure and year. Averages are taken across the full set of Monte Carlo simulation results from all 33 climate models, and all draws from the empirical distribution of estimated regression parameters, as described in Section 5.4. In panel B, the $25^{th}$-$75^{th}$ and $10^{th}$-$90^{th}$ percentile ranges of the Monte Carlo simulation distribution are shown for the mortality effects of climate change with benefits of income growth and adaptation (expression (iii)); the black line represents the same average value in both panels. Boxplots to the right summarize the distribution of mortality impacts for both RCP8.5 and the moderate emissions scenario of RCP4.5, and Figure F7 replicates the entire figure for RCP4.5.

Figure 6A illustrates that the mortality cost of climate change would be 221 deaths per 100,000 by 2100, on average across simulation runs (orange line), if the beneficial impacts of adaptation and income are shut down. This is a large estimate; if it were correct, the mortality costs of climate change would be roughly equivalent in magnitude to all global deaths from cardiovascular disease today (WHO, 2018).

However, we estimate that future income growth and adaptation to climate substantially reduce these

impacts, a finding that follows directly from the large gains to adaptation and income recovered in the historical record in Section 4. Higher incomes lower the mortality effect of climate change to an average of 104 deaths per 100,000 in 2100 (yellow line), although this estimate exhibits substantial uncertainty (Table D1, Figure F3). Climate adaptation reduces this further to 73 deaths per 100,000 (green line). Although much lower than the *no adaptation* projection, these smaller counts of direct mortality remain economically meaningful—for comparison, the 2019 mortality rate from automobile accidents in the United States was 11 per 100,000.

These large benefits of income growth and climate adaptation are driven by substantial changes in the mortality-temperature relationship over the $21^{st}$ century. For example, for the >64 age group, the average global increase in the mortality rate on a 35°C day (relative to a day at location-specific minimum mortality temperatures) declines by roughly 75% between 2015 and 2100, going from 10.1 per 100,000 to just 2.4 per 100,000 in 2100 (see Figure E2). Increasing incomes account for 77% of the decline, with adaptation to climate explaining the remainder; income gains account for 89% and 82% of the decline for the <5 and 5-64 categories, respectively.[30]

The values in Figure 6A are mean values aggregated across results from the 33 high-resolution climate models and all Monte Carlo simulation runs, but the full distribution of our estimated damages across climate models (panel B of Figure 6) is right-skewed. Indeed, there is meaningful mass in the "right" tail of potential mortality risk. As evidence of this, the *median* value of the mortality effects of climate change with benefits of income growth and adaptation under RCP8.5 at end of century is 42 deaths per 100,000, as compared to a *mean* value of 73, and the $10^{th}$ to $90^{th}$ percentile range is [-22, 197].

Figure 6B and Appendix Figure F5 display the expected implications of emissions mitigation. The average estimate of the mortality effects of climate change with benefits of income growth and adaptation of 73 deaths per 100,000 by the end of the century under RCP8.5 falls to 11 under the emissions stabilization scenario of RCP4.5 (where emissions decline after 2050). For RCP4.5, the median end-of-century estimate is 4, and the $10^{th}$ to $90^{th}$ percentile range is [-36, 62].

As a point of comparison to the limited literature estimating the global mortality consequences of climate change, we contrast these results to the FUND model, which is unique among the IAMs for calculating separate mortality impacts as a component of its SCC calculation. Although it is difficult to make a direct comparison due to differences in socioeconomic and emissions scenarios, different treatments of adaptation, and the inclusion of diarrhea and vector-borne diseases in FUND, the closest analog is to compare our estimates of the mortality impacts of climate change including adaptation benefits, a change of 73 deaths per 100,000 by 2100 under RCP8.5, to FUND's reference scenario change of 0.33 deaths per 100,000 in the same year (Anthoff and Tol, 2014).[31] The FUND model was calibrated decades ago based on limited mortality data from just 20 cities largely in wealthy and temperate locations; it is apparent that modern econometric tools and large-scale datasets provide a substantially different picture of the mortality consequences of climate

[30]These values apply to socioeconomic scenario SSP3.

[31]This value was calculated by running the MimiFUND model (v3.12.1) and extracting global additional deaths from all modeled causes. Additional deaths are calculated as the difference between the reference scenario in MimiFUND and a baseline in which both temperature and $CO_2$ are held constant at their 2005 levels. See Table B4 for details on the differences between our approach, that of FUND, and that of other empirical estimates of the impacts of climate change on mortality.

change.

Before proceeding, we note that a limitation of our empirical approach is that we must sometimes extrapolate response functions to temperatures outside of those historically observed within our data. To address the concern that out-of-sample behavior is disproportionately influencing our results, we repeat the projections of mortality risk changes with two extra sets of restrictions imposed upon our empirically-estimated response functions. These two restrictions, described in detail in Appendix F.3, are: *i)* forcing the response function to be flat for all temperatures outside the observed range, so that, for example, a 42°C day is no more damaging than a 40°C day; or *ii)* setting the marginal effect to be linearly increasing in the out-of-sample regions with a slope equal to the slope at the edge of the observed range. Figure F10 reveals that these two restrictions on out-of-sample behavior have negligible effects on our overall impacts. The value of the mortality impact of climate change including benefits of income growth and adaptation is approximately 1 death per 100,000 smaller by 2100 under RCP 8.5 in the case of the flat out-of-sample restriction (see Appendix F.3 for details).

# 6 The full value of the mortality risk of climate change

The empirical results above demonstrate that populations with similar incomes but different climates experience strikingly different mortality sensitivity to warming, with warmer populations benefiting from lower sensitivity to increasing heat. These differences reflect a wide variety of compensatory actions and, as highlighted in Equation 4 in Section 2, a full measure of the economic burden of climate change must account for these costs of adaptation. However, it is impossible to enumerate and observe all of the actions individuals take to modify their mortality risk of climate change.

This section develops a revealed preference approach that uses the observed differences in temperature sensitivity to infer measures of location-specific adaptation costs. Specifically, we assume that the differential mortality sensitivities to temperature are due to differential uptake of adaptive technologies, behaviors, or other investments. After all, if these investments were costless, we would expect universal uptake, such that mortality rates would exhibit little to no response to temperature across the globe. The approach therefore assumes that differences in the mortality sensitivity to temperature between locations can be the basis for inferring adaptation costs. This revealed preference approach relies on a strong set of simplifying assumptions, but it can be directly estimated with available data, even when the many dimensions of adaptation remain unobservable.

After outlining our approach for recovering adaptation costs, this section presents projections of the full mortality risk of climate change into the future, accounting for the benefits and costs of adaptation. We additionally demonstrate how the impacts of climate change on mortality and on mortality-related adaptation costs are projected to occur unequally across the globe.

## 6.1 Revealed preference approach to infer adaptation costs

As in Section 2, we define the the climate as the joint probability distribution over a vector of possible conditions that can be expected to occur over a specific interval of time. $\boldsymbol{C}_t$ describes this probability distribution in time period $t$ and $\boldsymbol{c}(\boldsymbol{C}_t)$ is a random vector of weather realizations drawn from the distribution characterized by $\boldsymbol{C}_t$.

Consider a single representative agent who derives utility in each time period $t$ from consumption of a numeraire good $x_t$. This agent faces mortality risk $f_t = f(\boldsymbol{b}_t, \boldsymbol{c}_t)$, which depends both on the weather and on adaptive behaviors and investments captured by the composite good $\boldsymbol{b}_t$. As discussed in Section 2, changes in the climate $\boldsymbol{C}$ influence mortality risk through altering weather realizations $\boldsymbol{c}$ and through changing beliefs about the weather, hence changing adaptive behaviors $\boldsymbol{b}$.

In bringing this framework to our empirical analysis (see Section 6.2 for details), we allow for 24,378 representative agents, one for each of the impact regions that together span the globe. We see this as a substantial improvement upon the existing estimates of global climate change damages that inform the SCC, even though there is heterogeneity in preferences, climate, and income within these regions. For example, the DICE IAM assumes a single homogeneous global region (Nordhaus, 1992), the RICE IAM assumes 10 homogeneous regions (Nordhaus and Yang, 1996), the FUND IAM assumes 16 homogeneous regions (Tol, 1997), and the empirically-derived SCC estimates in Ricke et al. (2018) are country-level.

Each region's representative agent simultaneously chooses consumption of the numeraire $x_t$ and of the composite good $\boldsymbol{b}_t$ in each period to maximize utility given her *expectations* of the weather, subject to an exogenous budget constraint and conditional on the climate. We let $\tilde{f}(\boldsymbol{b}_t, \boldsymbol{C}_t) = \mathbb{E}_{\boldsymbol{c}_t}[f(\boldsymbol{b}_t, \boldsymbol{c}(\boldsymbol{C}_t)) \mid \boldsymbol{C}_t]$ represent the expected probability of death. This agent therefore solves:

$$\max_{\boldsymbol{b}_t, x_t} \; u(x_t)\left[1 - \tilde{f}(\boldsymbol{b}_t, \boldsymbol{C}_t)\right] \quad s.t. \;\; Y_t \geq x_t + A(\boldsymbol{b}_t), \tag{6}$$

where $A(\boldsymbol{b}_t)$ represents expenditures for all adaptive investments, and $Y$ is an income we take to be exogenous. Under these assumptions, the first order conditions of Equation 6 define optimal adaptation as a function of income and the climate: $\boldsymbol{b}^*(Y_t, \boldsymbol{C}_t)$, which we sometimes denote below as $\boldsymbol{b}_t^*$ for simplicity.[32]

We use this framework to derive an empirically tractable expression for the full value of mortality risk due to climate change, following Equation 4. We begin by rearranging the agent's first order conditions and using the conventional definition of the VSL (i.e., $VSL = \frac{u(x)}{[1-\tilde{f}(\boldsymbol{b},\boldsymbol{C})]\partial u/\partial x}$ following, for example, Becker (2007) and Viscusi and Aldy (2003)[33]) to show that in any time period $t$,

$$\frac{\partial A(\boldsymbol{b}_t^*)}{\partial \boldsymbol{b}} = \frac{-u(x_t^*)}{\partial u/\partial x[1 - \tilde{f}(\boldsymbol{b}_t^*, \boldsymbol{C}_t)]} \frac{\partial \tilde{f}(\boldsymbol{b}_t^*, \boldsymbol{C}_t)}{\partial \boldsymbol{b}} = -VSL_t \frac{\partial \tilde{f}(\boldsymbol{b}_t^*, \boldsymbol{C}_t)}{\partial \boldsymbol{b}} \tag{7}$$

That is, marginal adaptation costs (lefthand side) equal the value of marginal adaptation benefits (righthand side), when evaluated at the optimal level of adaptation $\boldsymbol{b}^*$ and consumption $x^*$. This expression enables

[32] Note that income was omitted in the simplified motivation in Section 2, but enters as an argument of $\boldsymbol{b}_t^*$ here via the budget constraint.

[33] Note that this definition assumes the utility and marginal utility of consumption when dead is zero.

us to use estimates of marginal adaptation benefits, which we obtain from the previous section's estimation results, to infer estimates of marginal adaptation costs.

To make the expression in Equation 7 of greater practical value, we note that the total derivative of expected mortality risk with respect to a change in the climate is the sum of two terms:

$$\frac{d\tilde{f}(\boldsymbol{b}_t^*, \boldsymbol{C}_t)}{d\boldsymbol{C}} = \frac{\partial \tilde{f}(\boldsymbol{b}_t^*, \boldsymbol{C}_t)}{\partial \boldsymbol{b}} \frac{\partial \boldsymbol{b}_t^*}{\partial \boldsymbol{C}} + \frac{\partial \tilde{f}(\boldsymbol{b}_t^*, \boldsymbol{C}_t)}{\partial \boldsymbol{C}} \tag{8}$$

The first term on the righthand side of Equation 8 represents the expected impacts on mortality of all changes in adaptive investments induced by the change in climate; in practice, this term cannot be observed or estimated because of the countless elements of the $\boldsymbol{b}$ vector.[34] The second term is the direct effect that the climate would have if individuals did not adapt (i.e., the partial derivative).[35] If, as is expected, climate change produces an increase in the frequency of heat events that threaten human health, it would be natural to expect the first term to be negative, as people make adjustments that save lives. In this case, we expect the second term to be positive, reflecting the impacts of heat on fatalities absent those adjustment.

Equation 8 makes clear that we can express the unobservable mortality benefits of adaptation (i.e., $\frac{\partial \tilde{f}(\boldsymbol{b}_t^*, \boldsymbol{C}_t)}{\partial \boldsymbol{b}} \frac{\partial \boldsymbol{b}_t^*}{\partial \boldsymbol{C}}$) as the difference between the total and partial derivatives of the expected probability of death with respect to climate. This has important practical value because both of these terms can be estimated, as we describe below.

The combination of this algebraic manipulation with Equation 7 allows us to develop an expression for the *total* adaptation costs incurred as the climate changes gradually from $t_0$ to $t$ that is entirely composed of elements which can be estimated:[36]

$$A(\boldsymbol{b}^*(Y_t, \boldsymbol{C}_t)) - A(\boldsymbol{b}^*(Y_t, \boldsymbol{C}_{t_0})) = \int_{t_0}^{t} \frac{\partial A(\boldsymbol{b}_s^*)}{\partial \boldsymbol{b}} \frac{\partial \boldsymbol{b}_s^*}{\partial \boldsymbol{C}} \frac{d\boldsymbol{C}_s}{ds} ds = -\int_{t_0}^{t} VSL_s \left[ \frac{d\tilde{f}(\boldsymbol{b}_s^*, \boldsymbol{C}_s)}{d\boldsymbol{C}} - \frac{\partial \tilde{f}(\boldsymbol{b}_s^*, \boldsymbol{C}_s)}{\partial \boldsymbol{C}} \right] \frac{d\boldsymbol{C}_s}{ds} ds \tag{9}$$

Equation 9 outlines how we can use estimates of the total and partial derivatives of mortality risk—with respect to the climate—to infer marginal adaptation costs, even though adaptation itself is not directly observable. In the next subsection, we show how we use the empirical model described in Section 4 to separately identify the total derivative $\frac{d\tilde{f}}{d\boldsymbol{C}}$ and the partial derivative $\frac{\partial \tilde{f}}{\partial \boldsymbol{C}}$. We empirically quantify these values globally in Section 6.3.

A few details of this approach are worth underscoring. First, the *total* adaptation costs associated with the climate shifting from $\boldsymbol{C}_{t_0}$ to $\boldsymbol{C}_t$ are calculated by integrating marginal benefits of adaptation for a series of infinitesimal changes in climate (Equation 9), where marginal benefits continually evolve with the changing climate $\boldsymbol{C}$. Thus, total adaptation costs in a given period, relative to a base period, are the sum of the adaptation costs induced by a series of small changes in climate in the preceding periods (see Appendix A.1 for a visual description).

[34] This term is often known in the environmental health literature as the effect of "defensive behaviors" (Deschênes, Greenstone, and Shapiro, 2017) and in the climate change literature as "belief effects" (Deryugina and Hsiang, 2017); in our context these effects result from changes in individuals' defensive behaviors undertaken because their beliefs about the climate have changed.

[35] This term is known in the climate change literature as the "direct effect" of the climate (Deryugina and Hsiang, 2017).

[36] Note that $x$ is fully determined by $\boldsymbol{b}$ and income $Y$ through the budget constraint.

Second, the *total* adaptation benefits associated with the climate shifting from $\boldsymbol{C}_{t_0}$ to $\boldsymbol{C}_t$ are defined as the dollar value of the difference between the effects of climate change with optimal adaptation and without any adaptation: $-VSL_t[\tilde{f}(\boldsymbol{b}^*(Y_t, \boldsymbol{C}_t), \boldsymbol{C}_t) - \tilde{f}(\boldsymbol{b}^*(Y_t, \boldsymbol{C}_{t_0}), \boldsymbol{C}_t)]$. In contrast to total adaptation costs, this expression relies on the relationship between mortality and temperature that holds *only* at the final climate, $\boldsymbol{C}_t$. Therefore, when the marginal benefits of adaptation are greater at the final climate than at previous climates, the total benefits of adaptation will exceed total adaptation costs, generating an adaptation "surplus".[37] For example, at a climate between $\boldsymbol{C}_{t_0}$ and $\boldsymbol{C}_t$, the marginal unit of air conditioning (a key form of adaptation) purchased will have benefits that are exactly equal to its costs. However, at the warmer climate $\boldsymbol{C}_t$, this same unit of air conditioning becomes inframarginal, and is likely to have benefits that exceed its costs. Appendix A.2 derives a formal expression for this adaptation surplus.

Third, while we integrate over changes in climate in Equation 9, we hold income fixed at its endpoint value. This is because the goal is to develop an estimate of the additional adaptation expenditures incurred due to the changing climate only. In contrast, changes in expenditures due to rising income will alter mortality risk under climate change, but are not a consequence of the changing climate; therefore they are not included in our calculation of the total mortality-related costs of climate change.

Finally, this revealed preference approach is purposefully parsimonious so that it can be tightly linked to available data, but such simplification necessarily involves several strong assumptions. We assume that adaptation costs are a function of technology and do not depend on the climate, so that, for example, individuals in Seattle can purchase the same air conditioners as individuals in Houston can. We assume that $\tilde{f}(\cdot)$ is continuous and differentiable, that markets clear for all technologies and investments represented by the composite good $\boldsymbol{b}$, as well as for the numeraire good $x$, and that all choices $\boldsymbol{b}$ and $x$ can be treated as continuous. We assume that neither adaptation investments nor the climate directly enter the utility function, because the paper's focus is limited to the mortality risks of climate change.[38] Perhaps most importantly, the problem in Equation 6 is static. That is, we assume that there is a competitive and frictionless rental market for all capital goods (e.g., air conditioners), so that fixed costs of capital can be ignored, and that all rental decisions are contained in $\boldsymbol{b}$. While this rules out complementarities between adaptation decisions made by the representative agent in different time periods by assuming that such complementarities can be accommodated by sellers of adaptation services, it has to date been standard in the literature (e.g., Deryugina and Hsiang, 2017; Deschênes and Greenstone, 2011) and accounting for dynamic decision-making would necessitate an ambitious extension of the current paper.[39]

[37] Note that we derive an adaptation surplus assuming continuous adaptation investments $\boldsymbol{b}$; Guo and Costello (2013) find that adaptation surplus is higher when forward-looking agents invest in discrete adaptation behaviors or technologies.

[38] In an alternative specification detailed in Appendix A.4, we allow agents to derive utility both from $x$ and from the choice variables in $\boldsymbol{b}$; for example, air conditioning may increase utility directly, in addition to lowering mortality risk. Under this alternative framework, the costs of adapting to climate change that we can empirically recover, $A(\boldsymbol{b})$, are *net* of any changes in direct utility benefits or costs. Similarly, a model that assumes that climate enters utility directly would also lead to any adaptation costs associated with the direct effects of climate change being "netted out" in our approach to recovering adaptation costs.

[39] For example, the central contribution of Lemoine (2018) is to incorporate complementarity in adaptation actions across periods in a standard model of climate change impact estimation. This paper analyzes only a two-period complementarity, yet estimation in our context would require accurate weather forecast data for all locations and years in our estimating sample, a binding constraint for early years and in developing countries. It is also worth noting that the quantitative impacts of adding dynamic decision-making in Lemoine (2018) were minor, changing the end-of-century estimated losses to U.S. agriculture due to climate change from 47% under a static model to 50% under a dynamic model (see Table 2).

## 6.2 Computing adaptation costs using empirical estimates

To empirically estimate the adaptation costs incurred as the climate changes gradually from $t_0$ to $t$, following Equation 9, we calculate the following approximation (see Section A.3 for details):

$$\begin{aligned} A(\boldsymbol{b}^*(Y_t, \boldsymbol{C}_t))\widehat{-A}(\boldsymbol{b}^*(Y_t, \boldsymbol{C}_{t_0})) &\approx -\int_{t_0}^{t} VSL_s \left[\frac{d\hat{\bar{f}}(\boldsymbol{b}_s^*, \boldsymbol{C}_s)}{d\boldsymbol{C}} - \frac{\partial\hat{\bar{f}}(\boldsymbol{b}_s^*, \boldsymbol{C}_s)}{\partial\boldsymbol{C}}\right] \frac{d\boldsymbol{C}_s}{ds} ds \\ &\approx -\sum_{\tau=t_0+1}^{t} VSL_\tau \underbrace{\left(\frac{\partial \mathrm{E}[\hat{g}]}{\partial TMEAN}\bigg|_{\boldsymbol{C}_\tau, Y_t}\right)}_{\hat{\boldsymbol{\gamma}}_1 \mathrm{E}[\boldsymbol{T}]_\tau} (TMEAN_\tau - TMEAN_{\tau-1}), \end{aligned} \tag{10}$$

where the first line of Equation 10 is identical to Equation 9, except that we use "hat" notation to indicate that $\hat{\bar{f}}(\cdot)$ is an empirical estimate of expected mortality risk. The second (approximate) equality follows from (i) taking the total and partial derivative of our estimating equation (Equation 5) with respect to climate — where the total derivative accounts for adaptation while the partial does not, (ii) substituting terms and simplifying the expression, and (iii) implementing a discrete-time approximation for the continuous integral (see Appendix A.3 for a full derivation). The under-braced object, $\hat{\boldsymbol{\gamma}}_1 \mathrm{E}[\boldsymbol{T}]_\tau$, is the product of the expectation of temperature and the coefficient associated with the interaction between temperature and climate from our estimation of Equation 5: it represents our estimate of marginal adaptation benefits.[40] This derivative is then multiplied by the change in average temperature between each period.[41] Finally, we treat the VSL as a function of income, which evolves as incomes increase over time (see Section 7).

These adaptation cost estimates are calculated annually for each impact region and age group, as in Section 5, and for each of the 33 high-resolution climate model projections. These estimates enable us to develop a complete measure of the mortality costs of climate change that captures both the benefits and costs of adaptation. We continue to call this empirical estimate of Equation 4 the *full mortality risk of climate change*:

(iv) *Full mortality risk due to climate change* (including adaptation costs, recall Equation 4):

$$\begin{aligned} &\underbrace{\hat{g}(\boldsymbol{T}_t, TMEAN_t, \log(GDPpc)_t) - \hat{g}(\boldsymbol{T}_{t_0}, TMEAN_{t_0}, \log(GDPpc)_t)}_{\text{mortality effects of climate change with benefits of income growth and adaptation (iii)}} \\ &\quad + \underbrace{\frac{1}{VSL_t}\left[A(TMEAN_t, GDPpc_t)\widehat{-A}(TMEAN_{t_0}, GDPpc_t)\right]}_{\text{estimated adaptation costs}}. \end{aligned}$$

The adaptation cost term is multiplied by $\frac{1}{VSL}$ to convert it from dollars to lives. This conversion is important because it enables us to report the full mortality risk of climate change in a single unit, lives, rather than in lives and dollars. We note that using human lives serves as a natural numeraire in this revealed preference framework since we estimate adaptation costs based on lives that could be saved via adaptation, but are not.

[40] Recall that the specific functional form we use to estimate mortality risk as a function of temperature, climate, and income is $g(\cdot) = (\boldsymbol{\gamma}_0 + \boldsymbol{\gamma}_1 TMEAN_t + \boldsymbol{\gamma}_2 \log(GDPpc)_t)\,\boldsymbol{T}_t$. Thus, the partial derivative $\frac{\partial \mathrm{E}[\hat{g}]}{\partial TMEAN}$ is equivalent to $\hat{\boldsymbol{\gamma}}_1 \mathrm{E}[\boldsymbol{T}]_\tau$.

[41] We assume that individuals use the recent past to form expectations about current temperature realizations, so this expectation is computed over the prior 15 years, with weights of historical observations linearly declining in time.

We refer to these as "death equivalents", or the number of avoided deaths equal in value to the adaptation costs incurred.

## 6.3 Projections of the full mortality risk of climate change, accounting for adaptation benefits and costs

Table 2 summarizes the results for the full mortality risks of climate change at the end of the century, accounting for adaptation benefits and costs. The columns follow expressions (i)-(iv) detailed in Sections 5 and 6.2. Specifically, column 1 reports the mortality cost of climate change when the beneficial impacts of adaptation and income are shut down. Columns 2 and 3 show the change in mortality risk due to the benefits of income growth and climate adaptation, respectively; both reduce mortality, so the entries are negative. Column 4 presents estimates of adaptation costs in units of "death equivalents", following the calculation in Section 6.2. Finally, columns 5a and 5b show the full mortality risk of climate change, measured in deaths per 100,000 and monetized as a proportion of total global GDP in 2100.

### 6.3.1 Global estimates of the full mortality risk of climate change

Panel A of Table 2 shows mean estimates for the globe, averaging over a set of Monte Carlo simulations accounting for both climate and statistical uncertainty. The interquartile ranges across simulation runs are in brackets. Column 5a shows that, on average across the globe, the estimated full mortality risk due to climate change (i.e., expression (iv)) is projected to equal ∼85 deaths per 100,000 under RCP8.5 by 2100 (Appendix Figure F2 shows annual results over the century and Table F1 shows results for RCP4.5).[42] Of this full mortality risk, climate adaptation costs are estimated at ∼12 death equivalents per 100,000 (column 4), while increases in mortality rates account for the remaining 73 deaths per 100,000 (sum of columns 1 through 3). It is noteworthy that our estimate for the global average benefits of adaptation (column 3; 31 deaths per 100,000) exceeds the costs of these adjustments, demonstrating that the adaptation surplus of 19 deaths per 100,000 is substantial.[43]

[42] We previously noted considerable heterogeneity across age-groups in our results. We display the underlying age group heterogeneity of these projections in Appendix F.

[43] Appendix A.2 details the derivation of adaptation benefits and adaptation surplus.

**Table 2: Estimated 2100 full mortality risks of climate change, globally and regionally (high emissions scenario, RCP8.5)**

| | Mortality effects of climate change | | | | Full mortality risk of climate change | |
|---|---|---|---|---|---|---|
| | **No income growth or adaptation** | **Benefits of income growth** | **Benefits of climate adaptation** | **Costs of climate adaptation** | | |
| | *deaths/100k* | *deaths/100k* | *deaths/100k* | *deaths/100k* | *deaths/100k* | *% of GDP* |
| | (1) | (2) | (3) | (4) | (5a) | (5b) |
| **Panel A: Global estimates** | | | | | | |
| Mean Impacts | 220.6 | -116.5 | -31.0 | 11.7 | 84.8 | 3.2 |
| *IQR* | [76.4, 258.8] | [-149.4, -39.2] | [-60.1, 3.8] | [0.2, 19.4] | [17.4, 116.4] | [-5.4, 9.1] |
| **Panel B: Regional estimates** | | | | | | |
| China | 112.0 | -81.8 | -28.8 | 17.7 | 19.1 | 1.9 |
| USA | 14.8 | -13.2 | -1.8 | 10.2 | 10.1 | 1.0 |
| India | 334.4 | -248.2 | -25.6 | 2.1 | 62.7 | 6.0 |
| Pakistan | 589.1 | -161.7 | -105.0 | 53.6 | 376.0 | 27.5 |
| Bangladesh | 382.5 | -89.3 | -79.3 | 34.7 | 248.5 | 18.5 |
| Europe | -14.3 | -6.2 | -74.8 | 90.8 | -4.7 | 0.1 |
| Sub-Saharan Africa | 232.5 | -77.4 | -34.5 | 10.5 | 131.8 | 8.4 |

All columns show predicted mortality effects of climate change across all age categories and are represented by a mean estimate across a set of Monte Carlo simulations accounting for both climate model and statistical uncertainty. In the first row, brackets indicate the interquartile range (IQR). Columns 1-4 each indicate a partial mortality effect of climate change, in units of deaths per 100,000. Column 1 (expression (i)): mortality effects of climate change without benefits of income or adaptation to climate change. Column 2 (expression (ii) - expression (i)): benefits of income growth. Column 3 (expression (iii) - expression (ii)): benefits of adaptation to climate change. Column 4 (Equation 10): mortality-related costs of adaptation inferred using a revealed preference approach, measured in "death equivalents". Columns 5a-5b (expression (iv)): the full mortality risk of climate change, measured in deaths per 100,000 (column 5a) and represented as % of 2100 GDP (column 5b) using an age-adjusted value of the U.S. EPA VSL with an income elasticity of one applied to all impact regions. Column 5a is equivalent to the sum of columns 1 through 4. All estimates shown rely on the RCP8.5 emissions scenario and the SSP3 socioeconomic scenario. Table F1 shows equivalent results for SSP3 and RCP4.5 and details the regional definitions for Europe and sub-Saharan Africa.

Column 5b of Table 2 shows the monetized full mortality risk of climate change at the end of the century. To construct these estimates, we use the value of a statistical life (VSL) to convert changes in mortality rates into dollars. Our primary approach relies on the U.S. EPA's VSL estimate of $10.95 million (2019 USD).[44] We transform the VSL into a value per life-year lost using a method described in Appendix H.1, which allows us to compute the total value of expected life-years lost due to climate change, accounting for the different mortality-temperature relationships among the three age groups documented above. We allow the VSL to vary with income, as the level of consumption affects the relative marginal utilities of a small increment of consumption and a small reduction in the probability of death. Consistent with existing literature (e.g., Viscusi, 2015), our primary estimates use an income elasticity of unity to adjust the U.S. estimates of the VSL to different income levels across the world and over time.[45] When computing the mortality partial SCC in Section 7, we provide multiple alternative valuation assumptions in addition to this benchmark case.

The resulting estimates in column 5b are substantial. For example, under RCP8.5, they amount to 3.2% of global GDP in 2100, with an interquartile range of [-5.4%, 9.1%]. Under RCP4.5 (shown in Table F1), they fall to 0.6% [-3.9%, 4.6%] of global GDP. The uncertainty around these estimates is also meaningful and while we leave explicit pricing of this uncertainty to future work, accounting for it with a certainty equivalence-style calculation would only increase the estimated welfare loss from climate change.

These results suggest that the mortality risks from climate change are much greater than had previously been understood. For instance, these mortality-related damages amount to ∼49-135% of the damages reported for *all sectors of the economy* in FUND, PAGE, and DICE, when the damage functions from each model are evaluated at the mean end-of-century warming observed in our multi-model ensemble under RCP8.5. Under RCP4.5, our mortality-related damages amount to 32-61% of the damages from DICE and PAGE, while damages from FUND are negative at RCP4.5 levels of warming.[46]

The results in this and the previous section have relied on a single benchmark emissions and socioeconomic scenario (RCP8.5, SSP3). Appendix F reports on the sensitivity of the full mortality risk of climate change results to alternative choices about the economic and population scenario, the emissions scenario, and assumptions regarding the rate of adaptation. These exercises underscore that the projected impacts of climate change over the remainder of the $21^{st}$ century depend on difficult-to-predict factors such as policy, technology, and demographics. However, we note that under both emissions scenarios RCP8.5 and RPC4.5, under all SSP scenarios, and under an alternative projection in which the rate of adaptation is deterministically slowed, the average estimate of the full mortality risk due to climate change is positive (both RCPs) and steadily increasing (RCP8.5) throughout the $21^{st}$ century.

[44]This VSL is from the 2012 U.S. EPA Regulatory Impact Analysis (RIA) for the Clean Power Plan Final Rule, which provides a 2020 income-adjusted VSL in 2011 USD, which we convert to 2019 USD. This VSL is also consistent with income- and inflation-adjusted versions of the VSL used in the U.S. EPA RIAs for the National Ambient Air Quality Standards (NAAQS) for Particulate Matter (2012) and the Repeal of the Clean Power Plan (2019), among many other RIAs.

[45]The EPA considers a range of income elasticity values for the VSL, from 0.1 to 1.7 (U.S. Environmental Protection Agency, 2016b), although their central recommendations are 0.7 and 1.1 (U.S. Environmental Protection Agency, 2016). A review by Viscusi (2015) estimates an income-elasticity of the VSL of 1.1.

[46]To conduct this comparison, we use the damage functions reported for each IAM in the Interagency Working Group on Social Cost of Carbon (2010), which are indexed against warming relative to the pre-industrial climate. We evaluate each damage function at the mean end-of-century warming (4°C for RCP8.5 and 1.8°C for RCP4.5) across the SMME climate model ensemble used in our analysis, after adjusting warming to align pre-industrial temperature anomalies from the IAMs with the anomalies relative to 2001-2010 from our analysis (Lenssen et al., 2019). We note that these leading IAMs use different socioeconomic scenarios and climate models than those used throughout this paper.

### 6.3.2 Unequal distribution of mortality risk from climate change.

Panel B of Table 2 displays estimates of the end-of-century mortality risk of climate change for select countries and regions of the world. These results indicate that the full mortality risk caused by climate change varies substantially across the globe. Notably, monetized estimates in column 5b are very high in some regions, such as Pakistan and Bangladesh, where impacts amount to 27.5% and 18.5% of GDP, respectively.[47] The share of the full mortality risk that is due to actual deaths (first term in expression (iv)) versus compensatory investments (second term in expression (iv)) also differs across regions. Some locations suffer large increases in mortality rates, such as India, where 97% of the full mortality risk due to climate change is attributable to rising death rates. Other regions avoid excess mortality through expensive adaptation. For example, the U.S. is projected to benefit from a small decline in the mortality rate of -0.2 deaths per 100,000 at end of century, but is also projected to incur adaptation costs amounting to 10 death equivalents per 100,000.

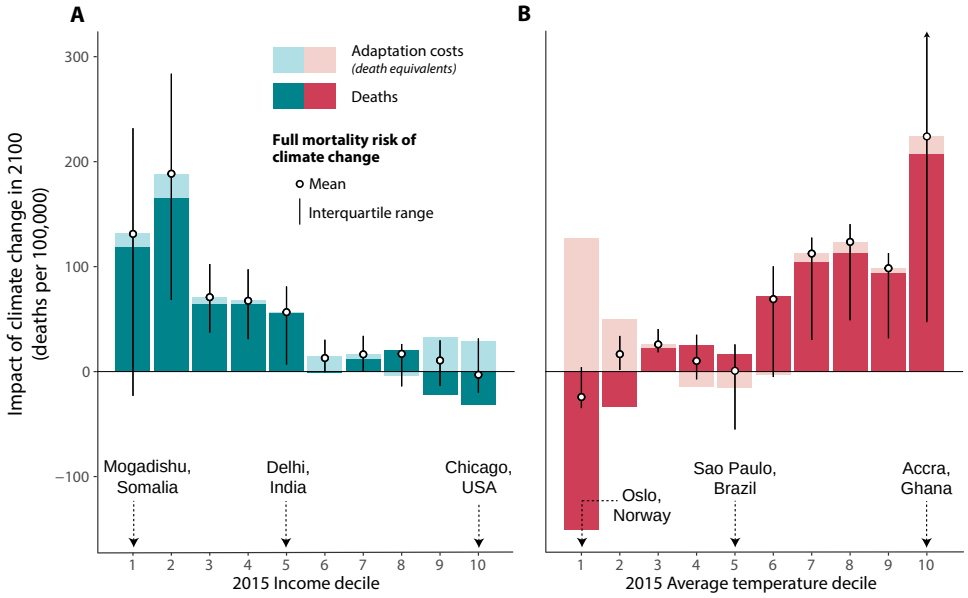


**Figure 7: Climate change impacts and adaptation costs are correlated with present-day income and climate.** Figure shows the mortality risk of climate change in 2100 (RCP8.5, SSP3) against deciles of 2015 per capita income (A) and average annual temperature (B). Dark colors indicate mean changes in death rates, accounting for the benefits of income growth and climate adaptation, while light colors indicate mean changes in adaptation costs, measured in death equivalents. For all bars shown, means are taken across impact regions falling into the corresponding decile of income or climate and across Monte Carlo simulations that account both for econometric and climate model uncertainty. Black outlined circles indicate the mean estimate of the full mortality risk of climate change, which is the sum of deaths and adaptation costs, and black vertical lines indicate the interquartile range of the distribution across impact regions within each decile. The income and average temperature deciles are calculated across 24,378 global impact regions and are population weighted using 2015 population values.

To visualize these distributional consequences, Figure 7 plots the full mortality risk of climate change in 2100 (dark bars), as well as the mean impact of climate change on adaptation costs (light bars), against deciles of present-day income (panel A) and present-day average temperature (panel B). These results reveal

[47]Note that Table 2 indicates that for Europe, the full mortality risk of climate change as measured in deaths per 100,000 (column 5a) is negative, while it is positive when measured in % of GDP (column 5b). This is because throughout much of Europe, climate change leads to lives being saved due to fewer extremely cold days, particularly for the >64 age group. Under the valuation approach shown in Table 2, an age-adjusted VSL is used, which lowers the relative weight placed on these lives saved in the older age group, as compared to increased mortality risk due to hot days in other age groups.

that the magnitude and composition of future mortality risks under climate change are strongly correlated with current incomes and climate. Panel A shows that the share of the full mortality risk due to adaptation costs is higher at higher incomes, indicating that wealthier locations are predicted to pay for future adaptive investments, while such costs are predicted to be much smaller in poor parts of the globe. In contrast, mortality rates are projected to increase much more dramatically in today's poor countries, indicating that climate impacts in these places will largely take the form of people living shorter lives. Further, the full mortality risk of climate change (shown in black and white circles) is still borne disproportionately by regions that are poor today. Finally, there is substantial variance across impact regions within each income decile, as shown by the interquartile range, underscoring the importance of geographic resolution in projecting climate impacts.

A similar figure in panel B demonstrates that the hottest locations today suffer the largest predicted increases in death rates, while the coldest are estimated to pay the highest adaptation costs. The magnitude of impacts in the top decile of the current long-run climate distribution are noteworthy and raise questions about the habitability of these locations at the end of the century.

# 7 The mortality partial social cost of carbon

This section uses the estimates of the full mortality risk of climate change to monetize the mortality-related social cost generated by emitting a marginal ton of $CO_2$. This calculation represents the component of the *total* SCC that is mediated through excess mortality, but it leaves out adverse impacts in other sectors of the economy, such as reduced labor productivity or changing food prices. Hence, it is a mortality *partial* SCC.

## 7.1 Definition: the mortality partial social cost of carbon

The mortality partial social cost of carbon at time $t$ is defined as the marginal social cost from the change in mortality risk imposed by the emission of a marginal ton of $CO_2$ in time period $t$. For a discount rate $\delta$, the mortality partial SCC is:

$$\textit{Mortality partial } SCC_t \text{ (dollars)} = \int_t^{\infty} e^{-\delta(s-t)} \frac{dD_s(\boldsymbol{C}_s)}{d\boldsymbol{C}} \frac{\partial \boldsymbol{C}_s}{\partial E_t} ds, \tag{11}$$

where $D_s(\boldsymbol{C}_s)$ represents a "damage function" describing *total* global economic losses (inclusive of both adaptation benefits and costs) due to changes in mortality risk in time period $s$, as a function of the global climate $\boldsymbol{C}$ (Nordhaus, 1992; Hsiang et al., 2017), and where $E_t$ represents total global greenhouse gas emissions in period $t$. $D_s(\cdot)$ varies over time, $s$, because the mortality sensitivity of temperature and total monetized impacts of climate change evolve over time due to changes in per capita income, the climate, and in the underlying population. Thus, the damages from a marginal change in emissions will vary depending on the year in which they are evaluated. In practice, we approximate Equation 11 by combining empirically grounded estimated damage functions $D_s(\cdot)$ with climate model simulations of the impact of a small change in emissions on the global climate, i.e., $\frac{\partial \boldsymbol{C}_s}{\partial E_t}$.

Expressing the mortality partial SCC using a damage function has three key practical advantages. First, the damage function represents a parsimonious, reduced-form description of the otherwise complex dependence of global economic damage on the global climate. Second, as we demonstrate below, it is possible to empirically estimate damage functions from the climate change projections described in Section 6. Finally, because they are fully differentiable, empirical damage functions can be used to compute *marginal* costs of an emissions impulse released in year $t$ by differentiation. The construction of these damage functions, as well as the implementation of the mortality partial SCC, are detailed in the following subsections.

## 7.2 Constructing damage functions for excess mortality risk

There are two key components of a damage function for excess mortality risk. First, the change in global mean surface temperature, $\Delta GMST_{rmt}$, which indicates the overall magnitude of warming. We compute this value for each of the two emissions scenarios $r$, each of the 33 climate models $m$, and each year $t$.[48] Second, total monetized losses due to changes in mortality risk, inclusive of adaptation benefits and cost, $D_{irmt}$, captures total damages for a given level of warming. We compute this value by summing projected estimates of the monetized full mortality risk of climate change across all 24,378 global impact regions, separately for each draw $i$ of the uncertain parameters recovered from estimation of the mortality-temperature relationship in Equation 5, emissions scenario $r$, climate model $m$, and year $t$. Therefore, for a given value of $\Delta GMST_{rmt}$, there is variation in damages $D_{irmt}$ due to econometric uncertainty captured by simulation runs $i$ and differential spatial distribution of warming across climate models.

Due to differences in the source of climate projections pre- and post-2100, and lack of available socioeconomic projections after 2100, there are some important methodological differences in how we estimate the relationship between damages $D_{irmt}$ and warming $\Delta GMST_{rmt}$ for years before versus after 2100. This subsection details these differences and also explains the approach to account for damage function uncertainty.

### 7.2.1 Computing damage functions through 2100.

For each year $t$ from 2020 to 2097, we estimate a set of quadratic damage functions that relate the total global value of mortality-related climate change damages ($D_{irmt}$) to the magnitude of global warming ($\Delta GMST_{rmt}$):

$$D_{irmt} = \alpha + \psi_{1,t}\Delta GMST_{rmt} + \psi_{2,t}\Delta GMST_{rmt}^2 + \varepsilon_{irmt}. \tag{12}$$

Specifically, to construct the damage function separately for each year $t$, we combine all 9,750 Monte Carlo simulation runs within a 5-year window centered on $t$ and estimate the regression in Equation 12.[49]This approach allows the recovered damage function $D_t(\Delta GMST)$ to evolve flexibly over the century. We note that pre-2100 damage functions are indistinguishable if we use a third-, fourth- or fifth-order polynomial, and we show robustness of our mortality partial SCC estimates to functional form choice in Appendix H.4.

[48]Our climate change impacts are calculated relative to a baseline of 2001-2010. Therefore, we define changes in global mean surface temperature ($\Delta GMST$) as relative to this same period. Note that the $\Delta GMST_{rmt}$ value in each climate model is a summary parameter, resulting from the complex interaction of many physical elements of the model, including the *equilibrium climate sensitivity*, a number that describes how much warming is associated with a specified change in greenhouse gas emissions.

[49]Because the projections in Section 6 end in 2100, 2097 is the last year for which a centered 5-year window of estimated damages can be constructed, and therefore is the last year for which we estimate Equation 12.

Figure 8A illustrates the procedure for the end-of-century damage function. Each data point plots a value of $D_{irmt}$ from an individual Monte Carlo simulation (vertical axis) against the corresponding value of $\Delta\text{GMST}_{rmt}$ (horizontal axis), where scatter points for years $t$=2095 through $t$=2100 are shown. Red points indicate simulation runs from the high emissions scenario ($r$=RCP8.5) and blue points indicate runs from the low emissions scenario ($r$=RCP4.5).[50] The median end-of-century warming relative to 2001-2010 under RCP8.5 across our climate models is +3.7°C, while under RCP4.5 it is +1.6°C. The black line is the end-of-century quadratic damage function, estimated following Equation 12.[51] The estimated damage function recovers total (undiscounted) damages with an age-varying VSL at 3.7°C and 1.6°C of $7.8 and $1.2 trillion USD, respectively. Analogous curves are constructed for all years, starting in 2020.

### 7.2.2 Computing post-2100 damage functions

Even with standard discount rates, a meaningful fraction of the present discounted value of damages from the release of $CO_2$ today will occur after 2100 (Kopp and Mignone, 2012), so it is important to develop post-2100 damage functions. The pre-2100 approach cannot be used for these later years because only 6 of the 21 GCMs that we use to build our SMME ensemble simulate the climate after 2100 for both RCP scenarios. Further, the SSPs needed to project the benefits of income growth and changes in demographic compositions also end in 2100.

To estimate post 2100-damages, we develop a method to extrapolate changes in the damage function beyond 2100 using the observed evolution of damages near the end of the $21^{st}$ century. The motivating principle of the extrapolation approach is that these observed changes in the shape of the damage function near the end of the century provide plausible estimates of future damage function evolution after 2100. This reduced-form approach allows our empirical results to constrain and guide a projection to years beyond 2100. To execute this extrapolation, we pool values $D_{irmt}$ from 2085-2100 and estimate a quadratic model similar to Equation 12, but interacting each term linearly with year $t$.[52] This allows estimation of a damage surface as a parametric function of year, which can then be used to predict extrapolated damage functions for all years after 2100, smoothly transitioning from our climate model-based damage functions prior to 2100. Appendix G provides a detailed explanation of the approach.

Panel B of Figure 8 illustrates damages functions every 10 years prior to 2100, as well as extrapolated damage functions for the years 2150, 2200, 2250, and 2300. In dollar terms, these extrapolated damages continue to rise post-2100, suggesting larger damages for a given level of warming. This finding comes directly from the estimation of Equation 12 that found that in the latter half of the $21^{\text{st}}$ century the full mortality damages are larger when they occur later, holding constant the degree of warming. This finding that mortality costs rise over time is the net result of countervailing forces. On the one hand, damages

[50] This scatterplot includes simulation runs for RCP4.5 and RCP8.5 for all projections in our 33-member ensemble under our benchmark method of valuation – the age-invariant EPA VSL with an income elasticity of one applied to all impact regions – in the end-of-century years 2095-2100. See Appendix H for results across different valuation assumptions. Due to the dependence of damages on GDP per capita and on demographics, we estimate separate damage functions following Equation 12 separately for every SSP scenario. Results across different scenarios are also shown in Appendix H.

[51] The damage function in Figure 8 is estimated for the year 2097, the latest year for which a full 5-year window of damage estimates can be constructed.

[52] We use 2085-2100 because the time evolution of damages becomes roughly linear conditional on $\Delta$GMST by this period.

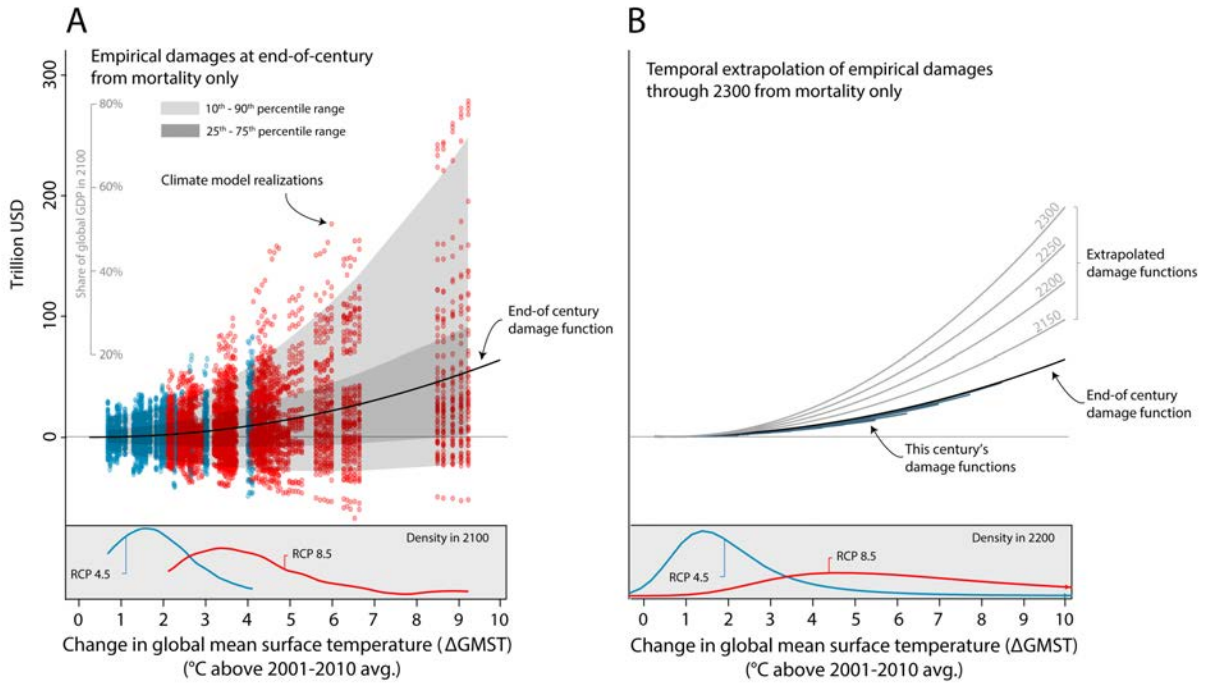


**Figure 8: Empirically-derived mortality-only damage functions.** Both panels show damage functions relating empirically-derived total global mortality damages to anomalies in global mean surface temperature (ΔGMST) under socioeconomic scenario SSP3. In panel A, each point (red = RCP8.5, blue = RCP4.5) indicates the value of the full mortality risk of climate change in a single year (ranging from 2095 to 2100) for a single simulation of a single climate model, accounting for both costs and benefits of adaptation. The black line is the quadratic damage function estimated through these points. The distribution of temperature anomalies at end of century (2095-2100) under two emissions scenarios across our 33 climate models is in the bottom panel. In panel B, the end-of-century damage function is repeated. Damage functions are shown in dark blue for every 10 years pre-2100, each of which is estimated analogously to the end-of-century damage function and is shown covering the support of ΔGMST values observed in the SMME climate models for the associated year. Our projection results generate mortality damages only through 2100, due to limited availability of climate and socioeconomic projections for years beyond that date. To capture impacts after 2100, we extrapolate observed changes in damages over the $21^{st}$ century to generate time-varying damage functions through 2300. The resulting damage functions are shown in light grey for every 50 years post-2100, each of which is extrapolated. The distribution of temperature anomalies around 2200 (2181-2200) under two emissions scenarios using the FAIR simple climate model is in the bottom panel. To value lives lost or saved, in both panels we use the age-varying U.S. EPA VSL and an income elasticity of one applied to all impact regions.

are larger in later years because there are larger and older populations[53] with higher VSLs due to rising incomes. On the other hand, damages are smaller in later years because populations are better adapted due to higher incomes and a slower rate of warming, enabling gradual adaptation. The results suggest the former dominates by end of century, causing damages to be trending upward when high-resolution simulations end in 2100. Below and in Appendix H, we explore the sensitivity of the results to alternative extrapolation approaches.

### 7.2.3 Accounting for uncertainty in damage function estimation.

As discussed, there is substantial uncertainty in projected mortality effects of climate change due to statistical uncertainty in the estimation of mortality-temperature response functions, as well as climate uncertainty arising from differences across the 33 climate models. The approach described above details the estimation

[53]In SSP3, the share of the global population in the >64 age category rises from 8.2% in 2015 to 16.2% in 2100.

of a damage function using the conditional expectation function through the full distribution of simulation results. In addition to reporting the predicted damages resulting from this damage function describing (conditional) expected values, we also estimate a set of quantile regressions to capture the full distribution of simulated mortality impacts.[54] Just as above for the mean damage function, extrapolation past the year 2100 is accomplished using a linear time interaction, estimated separately for each quantile. In the sections below, we use these quantiles to characterize uncertainty in the mortality partial SCC estimates. Thus, central estimates of the mortality partial SCC use the mean regression from Equation 12, while ranges incorporating damage uncertainty use the full set of time-varying quantile regressions.

## 7.3 Computing marginal damages from a marginal carbon dioxide emissions pulse

We empirically approximate the mortality partial SCC from Equation 11 for emissions that occur in the year 2020 as:

$$\textit{Mortality partial } SCC_{2020} \approx \sum_{t=2020}^{2300} e^{-\delta(t-2020)} \frac{\partial \hat{D}_t(\Delta GMST)}{\partial \Delta GMST} \frac{d\Delta GMST_t}{dCO2_{2020}}, \tag{13}$$

where $\Delta GMST$ approximates the multi-dimensional climate vector $\boldsymbol{C}$, and changes in $CO_2$ represent changes in global emissions $E$.[55] Additionally, we assume that discounted damages from an emissions pulse in year 2020 become negligible after 2300, and we approximate the integral in Equation 11 with a discrete sum using time steps of one year. The values $\frac{\partial \hat{D}_t(\Delta GMST)}{\partial \Delta GMST}$ are the marginal global damages in each year $t$ that occur as a result of this small change in all future global temperatures; they are computed using the damage functions described in the last subsection. The term $\frac{d\Delta GMST_t}{dCO2_{2020}}$ is the increase in $\Delta$GMST that occurs at each year $t$ along a baseline climate trajectory as a result of a marginal unit of emissions in 2020, which we approximate with an "infinitesimally small" pulse of $CO_2$ emissions. Because it is computationally infeasible to compute this value and account for uncertainty about the physical magnitude and timing of warming for all 33 climate models in the SMME, we use an alternative, global climate model to estimate $\frac{d\Delta GMST_t}{dCO2_{2020}}$, as detailed below.

### 7.3.1 Applying a simple climate model to the damage function.

To calculate the change in $\Delta\text{GMST}_t$ due to a marginal pulse of $CO_2$ in 2020, we use the Finite Amplitude Impulse Response (FAIR) simple climate model. We use FAIR to calculate $\Delta GMST_t$ trajectories for emissions scenarios RCP4.5 and RCP8.5, both with and without an exogenous "pulse" of 1 gigaton C (equivalent to 3.66Gt $CO_2$) in the year 2020, the smallest emission quantity for which a warming signal can be separated from noise within the FAIR climate model. In FAIR, this emissions pulse perturbs the trajectory of atmospheric $CO_2$ concentrations and $\Delta GMST$ for 2020-2300, with dynamics that are influenced by the baseline RCP scenario. In each emissions scenario, we then predict damages $\hat{D}_t(\Delta GMST_t)$ for $\Delta GMST$ values from

[54] We estimate a damage function for every $5^{th}$ percentile from the $5^{th}$ to $95^{th}$.

[55] We use $CO_2$ to represent changes in all global greenhouse gas (GHG) emissions as it is the most abundant GHG and the warming potential of all other GHGs are generally reported in terms of their $CO_2$ equivalence.

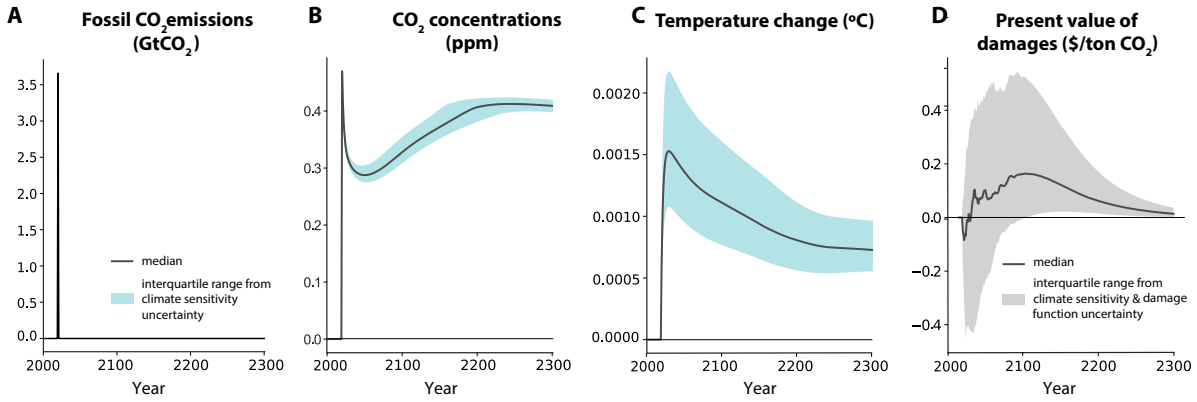


**Figure 9: Change in emissions, concentrations, temperature, and damages due to a marginal emissions pulse in 2020.** Panel A shows a 1GtC emissions pulse (equivalent to 3.66Gt $CO_2$) in 2020 for emissions scenario RCP8.5. Panel B displays the effect of this pulse on atmospheric $CO_2$ concentrations, relative to the baseline. In panel C, the impact of the pulse of $CO_2$ on temperature is shown where the levels are anomalies in global mean surface temperature (GMST) in Celsius. In panels A-C, shaded areas indicate the inter-quartile range due to climate sensitivity uncertainty, while solid lines are median estimates. Panel D shows the change in discounted damages over time due to a 1 Gt pulse of $CO_2$ in 2020 under socioeconomic scenario SSP3, as estimated by our empirically-derived damage functions, using a 2% annual discount rate and the age-varying U.S. EPA VSL with an income elasticity of one applied to all impact regions. The shaded area indicates the inter-quartile range due to climate sensitivity and damage function uncertainty, while the solid line is the median estimate.

the "RCP + pulse" simulation and difference them from predicted damages for $\Delta GMST$ values from the baseline "RCP only" simulation. The resulting damages due to the pulse are converted into USD per one metric ton $CO_2$. There is naturally uncertainty in these $\Delta GMST$ trajectories, and our approach accounts for uncertainty associated with four key parameters of the FAIR model (i.e., the transient climate response, equilibrium climate sensitivity, the short thermal adjustment time, and the time scale of rapid carbon uptake by the ocean mixed layer). This approach, detailed in Appendix G, ensures that the distribution of transient warming responses we use to generate partial SCC values matches the corresponding distributions from the IPCC Assessment Report 5 (AR5).

### 7.3.2 Summarizing the impacts of a marginal increase in $CO_2$ emissions.

Figure 9 graphically depicts the difference between the "RCP + pulse" and baseline RCP trajectories for four key outcomes.[56] The pulse in emissions is shown in panel A. Its influence on $CO_2$ concentrations is reported in panel B; the immediate decline followed by a century-long increase is largely due to dynamics involving the ocean's storage and release of emissions. Panel C displays the resulting change in temperature, which makes clear that a pulse today will influence temperatures even three centuries later. The solid lines are median estimates, while the shaded blue area in panels A-C depicts the inter-quartile range of each year's outcome, reflecting uncertainty about the climate system (see Appendix G for details).

Panel D plots the discounted (2% discount rate) stream of damages due to this marginal pulse of emissions. The temporal pattern of the present value of mortality damages reflects several factors, including: the nonlinearity of the damage function (e.g., Figure 8), which itself depends on nonlinearities in location-

[56]Using the trajectories in Figure 9 is consistent with the "SCC experiment" that is used in IAMs to calculate an SCC (National Academies of Sciences, Engineering, and Medicine, 2017). We discuss uncertainties in FAIR configuration parameters below and in Appendix G. The median values of parameter-specific distributions used for the central mortality partial SCC estimate include a transient climate response (TCR) of 1.6 and an equilibrium climate sensitivity (ECS) of 2.7.

specific mortality-temperature relationships (e.g., Figure 1); the discount rate; and the dynamic temperature response to emissions (panel C). The peak present value of annual damages from a ton of $CO_2$ emissions are \$0.16 in year 2104; by year 2277, annual damages are always less than \$0.02. It is noteworthy that about two-thirds of the present value of damages occur after the year 2100. The shaded grey area represents the inter-quartile range of each year's outcome, and reflects uncertainty in the climate system as well as uncertainty in the damage function. RCP4.5 results are shown in Figure G5 and additional details are in Appendix G.

### 7.4 Estimates of the partial social cost of carbon due to excess mortality risk

Table 3 reports mortality partial SCC estimates. The columns apply four different annual discount rates – three used in prior estimates of the SCC (2.5%, 3%, and 5%) (Interagency Working Group on Social Cost of Carbon, 2010; National Academies of Sciences, Engineering, and Medicine, 2017), and one lower rate that aligns more closely with recent global capital markets (2%) (Board of Governors of the US Federal Reserve System, 2020). Panel A uses the U.S. EPA's VSL of \$10.95 million (2019 USD), transformed into value per life-year lost (see Appendix H.1 for details). This accounts for the different mortality-temperature relationships among the three age groups documented above.[57] Panel B is based on an age-invariant value of \$10.95 million (2019 USD) for the VSL. Both approaches then adjust for cross sectional variation in incomes among contemporaries and global income growth. Appendix H presents results under a wide range of additional valuation scenarios, including an alternative and lower Ashenfelter and Greenstone (2004) VSL of \$2.39 million (2019 USD),[58] and an approach where the VSL is adjusted only based on global average income such that the lives of contemporaries are valued equally, regardless of their relative incomes.

The estimates in Table 3 utilize the median values of FAIR's four key parameter distributions and the mean global damage function. Interquartile ranges (IQRs) are reported, reflecting uncertainty in climate sensitivity (uncertainty in the simple climate model FAIR) and in the damage function. All values represent the global sum of each impact region's MWTP today (2019 USD) to avoid the release of an additional metric ton of $CO_2$ in 2020, including both the costs and benefits of adaptation.

Column 1 and panel A of Table 3 reports our preferred estimates of the mortality partial SCC. These are based on a $\delta = 2\%$ discount rate and an age-varying VSL. Under this valuation approach, the mortality partial SCC is \$17.1 [-\$24.7, \$53.6] for the low to moderate emissions scenario and \$36.6 [-\$7.8, \$73.0] for the high emissions scenario. We highlight a 2% discount rate because it conservatively reflects changes in global capital markets over the last several decades: while the Interagency Working Group on Social Cost of Greenhouse Gases (2016) recommends a discount rate of 3% based on the real 10-year Treasury rate calculated in 2003, the average 10-year Treasury Inflation-Indexed Security from 2003 to present is just 1.01% (Board of Governors of the US Federal Reserve System, 2020). We show results for a discount rate

[57] In the main text, a simple life-years calculation that assigns each life-year lost the same economic value is used. In Appendix H, we also show calculations that adjust the value of remaining life by age at death using the estimates of age-specific value of remaining life from Murphy and Topel (2006), which produces results that differ only slightly from those under the primary approach.

[58] See Appendix Table H1 for a comparison of these VSL values with values from the OECD, which are higher than Ashenfelter and Greenstone (2004), but lower than the U.S. EPA's VSL.

**Table 3: Estimates of a partial social cost of carbon for excess mortality risk incorporating the costs and benefits of adaptation**

| | Annual discount rate | | | |
|---|---|---|---|---|
| | $\delta = 2\%$ | $\delta = 2.5\%$ | $\delta = 3\%$ | $\delta = 5\%$ |
| **Panel A: Age-adjusted globally varying value of a statistical life (2019 US Dollars)** | | | | |
| Moderate emissions scenario (RCP4.5) | 17.1 | 11.2 | 7.9 | 2.9 |
| *Full uncertainty IQR* | [-24.7, 53.6] | [-18.9, 36.0] | [-15.2, 26.3] | [-8.5, 11.5] |
| High emissions scenario (RCP8.5) | 36.6 | 22.0 | 14.2 | 3.7 |
| *Full uncertainty IQR* | [-7.8, 73.0] | [-10.6, 46.8] | [-11.4, 32.9] | [-8.9, 13.0] |
| **Panel B: Globally varying value of a statistical life (2019 US Dollars)** | | | | |
| Moderate emissions scenario (RCP4.5) | 14.9 | 9.8 | 6.7 | 1.7 |
| *Full uncertainty IQR* | [-21.2, 63.5] | [-17.9, 43.5] | [-15.7, 32.1] | [-11.8, 14.7] |
| High emissions scenario (RCP8.5) | 65.1 | 36.9 | 22.1 | 3.5 |
| *Full uncertainty IQR* | [3.0, 139.0] | [-2.4, 83.1] | [-5.6, 53.4] | [-9.3, 16.0] |

In both panels, an income elasticity of one is used to scale the U.S. EPA VSL value (alternative values using the VSL estimate from (Ashenfelter and Greenstone, 2004) are shown in Appendix H). All regions thus have heterogeneous valuation, based on local income. All SCC values are for the year 2020, measured in PPP-adjusted 2019 USD, and are calculated from damage functions estimated from projected results under the socioeconomic scenario SSP3 (alternative values using other SSP scenarios are shown in Appendix H). In panel A, SCC estimates use an age adjustment that values deaths by the expected number of life-years lost, using an equal value per life-year (see Appendix H.1 for details and Appendix H.2 for alternative calculations that allow the value of a life-year to vary with age, based on Murphy and Topel (2006)). In panel B, SCC calculations use value of a statistical life estimates that do not vary with age. Point estimates rely on the median values of the four key input parameters into the climate model FAIR and a conditional mean estimate of the damage function. The uncertainty ranges are interquartile ranges [IQRs] including both climate sensitivity uncertainty and damage function uncertainty (see Appendix G for details).

of 1.5% in Appendix Table H4. We emphasize the age-varying VSL approach because standard economic reasoning implies that valuation of life lost should vary by age (Jones and Klenow, 2016; Murphy and Topel, 2006).

When following the Interagency Working Group on Social Cost of Greenhouse Gases (2016) preference for a discount rate of $\delta = 3\%$ and the use of an age-invariant VSL, the central estimate of the mortality partial SCC is \$6.7 per metric ton of $CO_2$ for the low to moderate emissions scenario (RCP4.5), with an IQR of [-\$15.7, \$32.1], and \$22.1 [-\$5.6, \$53.4] per metric ton for the high emissions scenario (RCP8.5).

Some other features of these results are worth underscoring. First, mortality partial SCC estimates for RCP4.5 are systematically lower than RCP8.5 primarily because the damage function is convex, so marginal damages increase in the high emissions scenario. Second, the combination of this convexity, which itself is accentuated at higher quantiles of the damage function, and the skewness of the climate sensitivity distribution causes the distribution of partial SCCs to also be right skewed with a long right tail. For example, the $95^{th}$ and $99^{th}$ percentiles of the partial SCC for $\delta = 2\%$ and an age-varying VSL for RCP8.5 are \$290.3 and \$704.1, respectively; with $\delta = 3\%$ and an age-invariant VSL these values are \$175.3 and \$391.9. It is apparent that a certainty equivalent estimate of the mortality partial SCC based on standard assumptions of risk aversion, which is beyond the scope of this paper, would be much larger than the mean estimates reported here. Third, in Appendix G we show that uncertainty in the partial SCC is consistently dominated

by uncertainty in the damage function, as opposed to uncertainty in climate sensitivity. Fourth, all mortality partial SCC estimates shown in the main text rely on an exogenous socioeconomic trajectory; in Table H6 we show that endogenizing impacts of climate change on income growth based on prior literature (Burke, Hsiang, and Miguel, 2015) has only a small effect on our mortality partial SCC results. Fifth, in Appendix H we show that replacing the extrapolation of damage functions to years beyond 2100 with a damage function frozen at its 2100 shape for all years 2101-2300 lowers our central estimate of the mortality partial SCC by 21%. This indicates that damage function extrapolation has a modest impact on our partial SCC estimates, due in part to the important role of discounting (Table H7). Finally, while Table 3 reflects what we believe to be mainstream valuation and socioeconomic scenarios, Appendix Tables H2-H8 report estimates based on multiple alternative approaches. Naturally, the resulting SCC estimates vary under different valuation assumptions and baseline socioeconomic trajectories, and we point readers to these specifications for a more comprehensive set of results.

# 8 Limitations

As the paper has detailed, the mortality risk changes from climate change and the mortality partial SCC have many ingredients. We have tried to probe the robustness of the results to each of them, but there are three issues that merit special attention when interpreting the results, because they are outside the scope of the analysis.

### 8.0.1 Migration Responses.

First, the estimates in the paper do not reflect the possibility of migration responses to climate change. If migration were costless, it seems likely that the full mortality risk and mortality partial SCC would be smaller, as people from regions with high damages (e.g., sub-Saharan Africa) may move to regions with low or even negative damages (e.g., Scandinavia). However, both distant and recent history in the U.S. and around the globe underscores that borders are meaningful and that there are substantial costs to migration which might limit the scale of feasible migrations. Indeed, existing empirical evidence of climate-induced migration, based on observable changes in climate to date, is mixed (Carleton and Hsiang, 2016).

### 8.0.2 Humidity.

Second, our estimates do not directly incorporate the role of humidity in historical mortality-temperature relationships nor in projections of future impacts. There is growing evidence that humidity influences human health through making it more difficult for the human body to cool itself during hot conditions (e.g., Sherwood and Huber, 2010; Barreca, 2012). While temperature and humidity are highly correlated over time, they are differentially correlated across space, implying that our measures of heterogeneous mortality-temperature relationships may be influenced by the role of humidity. To date, lack of high-resolution historical humidity data and highly uncertain projections of humidity under climate change (Sherwood and Fu, 2014) have limited our ability to include this heterogeneity in our work. However, emerging work on this topic (Yuan,

Stein, and Kopp, 2019; Li, Yuan, and Kopp, 2020) will provide opportunities to explore humidity in future research.

#### 8.0.3 Technological Change.

Third, the paper's projections incorporate advancements in technology that enhance adaptive ability, even though we have not explicitly modeled technological change. In particular, we allow mortality-temperature response functions to evolve in accordance with rising incomes and temperatures and do not restrict them to stay within the bounds of the current observed distribution of temperature responses. However, while our estimates reflect technical advancement as it historically relates to incomes and climate, they do not reflect the seemingly high probability of climate-biased technical change that lowers the *relative* costs of goods which reduce the health risks of high temperatures. Therefore, the paper's results will overstate the mortality risk of climate change if directed technological innovations lower the relative costs of adapting to high temperatures.

## 9 Conclusion

This paper has outlined a new method for empirically estimating the global costs of climate change for a single sector of the economy using micro data. We have implemented this approach in the context of mortality risks associated with temperature change. Specifically, this paper develops a framework for estimating the annual total impact of climate change on mortality risk, accounting for the benefits and costs of adaptation, both globally and for 24,378 regions that comprise the planet. It then uses these estimates to compute a mortality "partial" SCC, defined as the global marginal willingness-to-pay to avoid the changes in mortality risk caused by the release of an additional metric ton of $CO_2$.

There are three noteworthy methodological innovations and key findings. First, we leverage highly resolved data covering roughly half of the world's population to estimate flexible empirical models relating mortality rates to temperature. These regressions uncover a plausibly causal U-shaped relationship where extreme cold and hot temperatures increase mortality rates, especially for those aged 65 and older. Moreover, this relationship is quite heterogeneous across the planet as both income and long-run climate substantially moderate mortality sensitivity to temperature. Further when combined with current global data on climate, income, and population, the results imply that the effect of a hot day (35°C / 95°F) on mortality in the >64 age group is ∼50% larger in regions of the world without available mortality data. This suggests that prior estimates from wealthy economies and temperature climates are likely to understate the impacts of climate change on human mortality.

Second, we use these regression results along with future projections of climate, income, and population to estimate future climate change-induced mortality risk both in terms of fatality rates and its monetized value. We find that, under a high emissions scenario, the projected impact of climate change on mortality will be comparable globally to leading causes of death today, such as cancer and infectious disease (Figure 10). We also estimate large benefits from mitigation, as the end of century estimate of the full mortality risk of climate change falls from 85 deaths per 100,000 under the high emissions growth RCP8.5 scenario to 14

per 100,000 under the more moderate RCP4.5 scenario. Importantly, these projected impacts include the benefits of adaptation to gradual climate change; estimates that do not account for adaptation overstate the mortality impacts of climate change in 2100 by more than a factor of about 3. Additionally, we outline and implement a revealed preference method to infer the costs of these adaptation investments, which amount to, on average, 12 death equivalents per 100,000 out of the total of 85 deaths per 100,000 in 2100 in the RCP8.5 scenario.

Further, the estimated mortality-related damages from climate change are distributed unevenly across the world. For example, by 2100, we project that climate change will cause annual damages equivalent to approximately 160 additional deaths per 100,000 in Accra, Ghana, but will also generate annual benefits equivalent to approximately 9 lives per 100,000 in London, England. Notably, the degree to which the full mortality risk of climate change is realized through actual deaths, as opposed to costly adaptation, varies widely across space and time. For example, Figure 10 shows that today's poor locations tend to bear a larger share of the projected burden in the form of direct mortality impacts, while today's rich face large increases in projected adaptation costs.

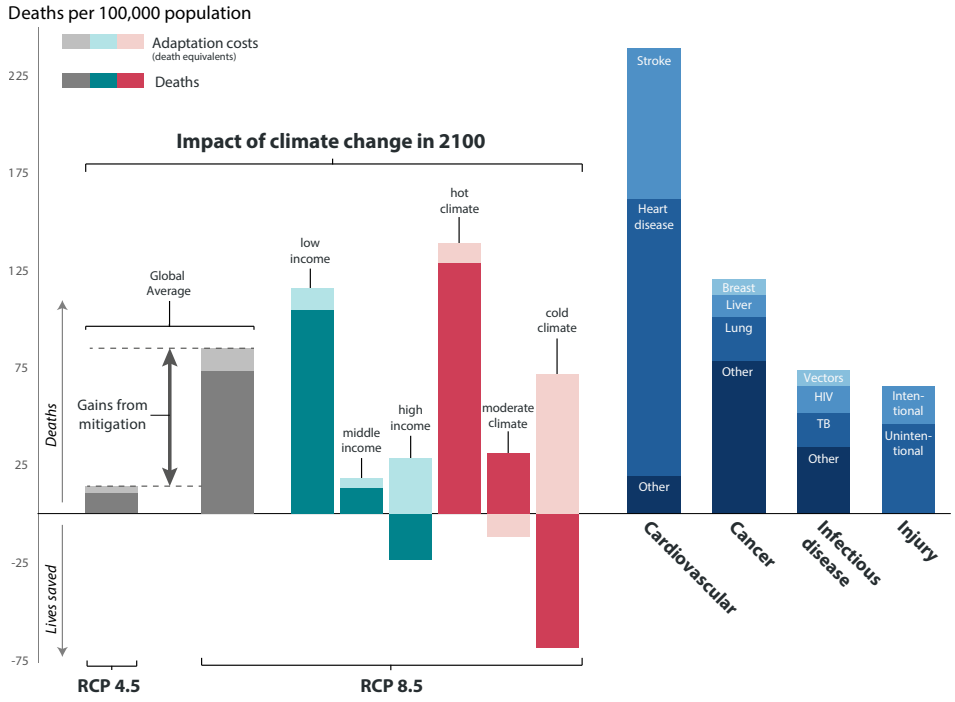


**Figure 10: The impact of climate change in 2100 is comparable to contemporary leading causes of death.** Impacts of climate change (grey, teal, and coral) are calculated for the year 2100 for socioeconomic scenario SSP3 and include changes in death rates (solid colors) and changes in adaptation costs, measured in death equivalents (light shading). Global averages for RCP 8.5 and RCP 4.5 are shown in grey, demonstrating the gains from mitigation. Income and average climate groups under RCP8.5 are separated by tercile of the 2015 global distribution across all 24,378 impact regions. Blue bars on the right indicate average mortality rates globally in 2018, with values from WHO (2018). Figure F8 provides an RCP4.5 version of this figure.

Finally, we use these projections to develop the first empirically grounded estimates of the mortality partial SCC. Using a 2% discount rate and age-varying VSL, the 2020 mortality partial SCC is roughly

$36.6 (in 2019 USD) with a high emissions scenario and $17.1 with a moderate one. There is substantial uncertainty around these estimates, arising both from climate sensitivity and damage function uncertainty. For example, the interquartile ranges of the mortality partial SCC are [-$7.8, $73.0] and [-$24.7, $53.6], under high and moderate emissions scenarios, respectively. These ranges underscore the nature of the climate challenge and highlight that, while beyond the scope of this paper, valuing this uncertainty under risk aversion will raise the mortality partial SCC.

Overall, the paper's findings suggest that previous research has significantly understated climate change damages due to mortality. For example, the mortality damages we estimate in 2100 account for 49% to 135% of *total* damages across all sectors of the economy according to leading IAMs. Moreover, the mortality partial SCC reported here, under comparable valuation assumptions, is more than 10 times larger than the total health impacts embedded in the FUND IAM (Diaz, 2014).[59]

We believe that this paper has highlighted a key role for systematic empirical analysis in providing a clearer picture of the magnitude of the costs of climate change and how, why, and where they are likely to emerge in the future. Advances in access to data and computing have removed the need to rely so heavily on assumptions when estimating the economic costs of climate change. Looking ahead, the paper's general approach can be applied to other aspects of the global economy besides mortality risk, and doing so is a promising area for future research.

[59]Diaz (2014) computes comparable partial SCC values for FUND ($\delta = 3\%$, "business as usual" emissions) and reports values for three comparable health impacts (diarrhea, vector borne diseases, and cardiopulmonary) that total less than $2 (2019 USD).

# References


Alesina, Alberto and Dani Rodrik. 1994. "Distributive politics and economic growth." *The quarterly journal of economics* 109 (2):465–490.

Anthoff, David and Richard SJ Tol. 2014. "The climate framework for uncertainty, negotiation and distribution (FUND): Technical description, version 3.6." *FUND Doc* .

Ashenfelter, Orley and Michael Greenstone. 2004. "Using mandated speed limits to measure the value of a statistical life." *Journal of Political Economy* 112 (S1):S226–S267.

Auffhammer, Maximilian. 2018. "Climate adaptive response estimation: Short and long run impacts of climate change on residential electricity and natural gas consumption using big data." *NBER Working paper* .

Auffhammer, Maximilian and Anin Aroonruengsawat. 2011. "Simulating the impacts of climate change, prices and population on California's residential electricity consumption." *Climatic Change* 109 (1):191–210. URL http://dx.doi.org/10.1007/s10584-011-0299-y.

Bailey, Martha J and Andrew Goodman-Bacon. 2015. "The War on Poverty's experiment in public medicine: Community health centers and the mortality of older Americans." *American Economic Review* 105 (3):1067–1104.

Barreca, Alan, Karen Clay, Olivier Deschênes, Michael Greenstone, and Joseph S Shapiro. 2015. "Convergence in adaptation to climate change: Evidence from high temperatures and mortality, 1900–2004." *The American Economic Review* 105 (5):247–251.

Barreca, Alan, Karen Clay, Olivier Deschenes, Michael Greenstone, and Joseph S. Shapiro. 2016. "Adapting to climate change: The remarkable decline in the US temperature-mortality relationship over the twentieth century." *Journal of Political Economy* 124 (1):105–159. URL http://dx.doi.org/10.1086/684582.

Barreca, Alan I. 2012. "Climate change, humidity, and mortality in the United States." *Journal of Environmental Economics and Management* 63 (1):19–34.

Becker, Gary S. 2007. "Health as human capital: synthesis and extensions." *Oxford Economic Papers* 59 (3):379–410.

Board of Governors of the US Federal Reserve System. 2020. "10-Year Treasury Inflation-Indexed Security, Constant Maturity [DFII10]." Tech. rep., FRED, Federal Reserve Bank of St. Louis. URL https://fred.stlouisfed.org/series/DFII10.

Bright, E. A., P. R. Coleman, A. N. Rose, and M. L. Urban. 2012. "LandScan 2011." Digital dataset: web.ornl.gov/sci/landscan/index.shtml.

Burgess, Robin, Olivier Deschenes, Dave Donaldson, and Michael Greenstone. 2017. "The unequal effects of weather and climate change: Evidence from mortality in India." *NBER Working paper* .

Burke, Marshall, John Dykema, David B Lobell, Edward Miguel, and Shanker Satyanath. 2015. "Incorporating climate uncertainty into estimates of climate change impacts." *Review of Economics and Statistics* 97 (2):461–471.

Burke, Marshall, Solomon M Hsiang, and Edward Miguel. 2015. "Global non-linear effect of temperature on economic production." *Nature* 527 (7577):235–239.

Carleton, Tamma A and Solomon M Hsiang. 2016. "Social and economic impacts of climate." *Science* 353 (6304):aad9837.

Center for Systemic Peace. 2020. "Polity5: Political Regime Characteristics and Transitions 1800-2018." URL http://www.systemicpeace.org/inscrdata.html.

Davis, Lucas W and Paul J Gertler. 2015. "Contribution of air conditioning adoption to future energy use under global warming." *Proceedings of the National Academy of Sciences* 112 (19):5962–5967.

Dellink, Rob, Jean Chateau, Elisa Lanzi, and Bertrand Magné. 2015. "Long-term economic growth projections in the Shared Socioeconomic Pathways." *Global Environmental Change* .

Deryugina, Tatyana and Solomon Hsiang. 2017. "The Marginal Product of Climate." *NBER Working paper* .

Deschenes, Olivier. 2018. "Temperature Variability and Mortality: Evidence from 16 Asian Countries." *Asian Development Review* 35 (2):1–30.

Deschênes, Olivier and Michael Greenstone. 2007. "The economic impacts of climate change: evidence from agricultural output and random fluctuations in weather." *The American Economic Review* 97 (1):354–385.

———. 2011. "Climate change, mortality, and adaptation: Evidence from annual fluctuations in weather in the US." *American Economic Journal: Applied Economics* 3 (October):152–185. URL http://www.nber.org/papers/w13178.

Deschênes, Olivier, Michael Greenstone, and Joseph S Shapiro. 2017. "Defensive investments and the demand for air quality: Evidence from the NOx budget program." *American Economic Review* 107 (10):2958–89.

Deschênes, Olivier and Enrico Moretti. 2009. "Extreme weather events, mortality, and migration." *The Review of Economics and Statistics* 91 (4):659–681.

Diaz, Delavane. 2014. "Evaluating the Key Drivers of the US Government's Social Cost of Carbon: A Model Diagnostic and Inter-Comparison Study of Climate Impacts in DICE, FUND, and PAGE." *Working paper* .

Eurostat. 2013. *Europe in Figures: Eurostat Yearbook 2013*. Publications Office of the European Union.

Fetzer, Thiemo. 2014. "Can workfare programs moderate violence? Evidence from India." .

Friedman, Jerome, Trevor Hastie, Robert Tibshirani et al. 2001. *The elements of statistical learning*, vol. 1. Springer series in statistics New York.

Gasparrini, Antonio, Yuming Guo, Masahiro Hashizume, Eric Lavigne, Antonella Zanobetti, Joel Schwartz, Aurelio Tobias, Shilu Tong, Joacim Rocklöv, Bertil Forsberg et al. 2015. "Mortality risk attributable to high and low ambient temperature: A multicountry observational study." *The Lancet* 386 (9991):369–375.

Gennaioli, Nicola, Rafael La Porta, Florencio Lopez De Silanes, and Andrei Shleifer. 2014. "Growth in regions." *Journal of Economic Growth* 19 (3):259–309. URL https://ideas.repec.org/a/kap/jecgro/v19y2014i3p259-309.html.

Glaeser, Edward L, Rafael La Porta, Florencio Lopez-de Silanes, and Andrei Shleifer. 2004. "Do institutions cause growth?" *Journal of economic Growth* 9 (3):271–303.

Graff Zivin, Joshua and Matthew Neidell. 2014. "Temperature and the allocation of time: Implications for climate change." *Journal of Labor Economics* 32 (1):1–26.

Guo, Christopher and Christopher Costello. 2013. "The value of adaption: Climate change and timberland management." *Journal of Environmental Economics and Management* 65 (3):452–468.

Guo, Yuming, Antonio Gasparrini, Ben Armstrong, Shanshan Li, Benjawan Tawatsupa, Aurelio Tobias, Eric Lavigne, Micheline de Sousa Zanotti Stagliorio Coelho, Michela Leone, Xiaochuan Pan et al. 2014. "Global variation in the effects of ambient temperature on mortality: a systematic evaluation." *Epidemiology (Cambridge, Mass.)* 25 (6):781.

Heutel, Garth, Nolan H Miller, and David Molitor. 2017. "Adaptation and the Mortality Effects of Temperature Across US Climate Regions." *National Bureau of Economic Research* .

Houser, Trevor, Solomon Hsiang, Robert Kopp, Kate Larsen, Michael Delgado, Amir Jina, Michael Mastrandrea, Shashank Mohan, Roger Muir-Wood, DJ Rasmussen, James Rising, and Paul Wilson. 2015. *Economic risks of climate change: An American prospectus*. Columbia University Press.

Hsiang, Solomon. 2013. "Visually-weighted regression." *SSRN Working Paper* .

———. 2016. "Climate econometrics." *Annual Review of Resource Economics* 8:43–75.

Hsiang, Solomon, Robert Kopp, Amir Jina, James Rising, Michael Delgado, Shashank Mohan, DJ Rasmussen, Robert Muir-Wood, Paul Wilson, Michael Oppenheimer et al. 2017. "Estimating economic damage from climate change in the United States." *Science* 356 (6345):1362–1369.

Hsiang, Solomon M and Amir S Jina. 2014. "The causal effect of environmental catastrophe on long-run economic growth: Evidence from 6,700 cyclones." Tech. rep., National Bureau of Economic Research.

Hsiang, Solomon M, Kyle C Meng, and Mark A Cane. 2011. "Civil conflicts are associated with the global climate." *Nature* 476 (7361):438.

Hsiang, Solomon M and Daiju Narita. 2012. "Adaptation to cyclone risk: Evidence from the global cross-section." *Climate Change Economics* 3 (02):1250011.

IIASA Energy Program. 2016. "SSP Database, Version 1.1 [Data set]." Tech. rep., National Bureau of Economic Research. URL https://tntcat.iiasa.ac.at/SspDb.Accessed25December,2016.

Interagency Working Group on Social Cost of Carbon. 2010. "Social Cost of Carbon for Regulatory Impact Analysis - Under Executive Order 12866." Tech. rep., United States Government.

Interagency Working Group on Social Cost of Greenhouse Gases. 2016. "Technical Support Document: Technical Update of the Social Cost of Carbon for Regulatory Impact Analysis." Tech. rep., United States Government.

Isen, Adam, Maya Rossin-Slater, and Reed Walker. 2017. "Relationship between season of birth, temperature exposure, and later life wellbeing." *Proceedings of the National Academy of Sciences* 114 (51):13447–13452.

Jones, Charles I and Peter J Klenow. 2016. "Beyond GDP? Welfare across countries and time." *American Economic Review* 106 (9):2426–57.

Kahn, Matthew E. 2005. "The death toll from natural disasters: the role of income, geography, and institutions." *Review of Economics and Statistics* 87 (2):271–284.

Kelly, David L, Charles D Kolstad, and Glenn T Mitchell. 2005. "Adjustment costs from environmental change." *Journal of Environmental Economics and Management* 50 (3):468–495.

Kopp, Robert E and Bryan K Mignone. 2012. "The US government's social cost of carbon estimates after their first two years: Pathways for improvement." *Working paper* .

La Porta, Rafael and Andrei Shleifer. 2014. "Informality and development." *Journal of Economic Perspectives* 28 (3):109–26.

Lemoine, Derek. 2018. "Estimating the consequences of climate change from variation in weather." Tech. rep., National Bureau of Economic Research.

Lenssen, N., G. Schmidt, J. Hansen, M. Menne, A. Persin, R. Ruedy, and D. Zyss. 2019. "Improvements in the GISTEMP uncertainty model." *J. Geophys. Res. Atmos.* 124 (12):6307–6326.

Li, Dawei, Jiacan Yuan, and Robert Bob Kopp. 2020. "Escalating global exposure to compound heat-humidity extremes with warming." *Environmental Research Letters* .

Matsuura, Kenji and Cort Willmott. 2007. "Terrestrial Air Temperature and Precipitation: 1900-2006 Gridded Monthly Time Series, Version 1.01." *University of Delaware*. URL http://climate.geog.udel.edu/climate.

Mendelsohn, Robert, William D Nordhaus, and Daigee Shaw. 1994. "The impact of global warming on agriculture: A Ricardian analysis." *The American Economic Review* :753–771.

Millar, Richard J, Zebedee R Nicholls, Pierre Friedlingstein, and Myles R Allen. 2017. "A modified impulse-response representation of the global near-surface air temperature and atmospheric concentration response to carbon dioxide emissions." *Atmospheric Chemistry and Physics* 17 (11):7213–7228.

Moore, Frances C and David B Lobell. 2014. "Adaptation potential of European agriculture in response to climate change." *Nature Climate Change* 4 (7):610.

Murphy, Kevin M and Robert H Topel. 2006. "The value of health and longevity." *Journal of Political Economy* 114 (5):871–904.

National Academies of Sciences, Engineering, and Medicine. 2017. *Valuing Climate Damages: Updating Estimation of the Social Cost of Carbon Dioxide*. Washington, DC: The National Academies Press. URL https://www.nap.edu/catalog/24651/valuing-climate-damages-updating-estimation-of-the-social-cost-of.

Nordhaus, William D. 1992. "An optimal transition path for controlling greenhouse gases." *Science* 258 (5086):1315–1319.

Nordhaus, William D and Zili Yang. 1996. "A regional dynamic general-equilibrium model of alternative climate-change strategies." *The American Economic Review* :741–765.

Organization of Economic Cooperaton and Development. 2020. "OECD.Stat." URL https://doi.org/10.1787/data-00285-en.

Rasmussen, D. J., Malte Meinshausen, and Robert E. Kopp. 2016. "Probability-weighted ensembles of U.S. county-level climate projections for climate risk analysis." *Journal of Applied Meteorology and Climatology* 55 (10):2301–2322. URL http://journals.ametsoc.org/doi/abs/10.1175/JAMC-D-15-0302.1.

Riahi, Keywan, Detlef P Van Vuuren, Elmar Kriegler, Jae Edmonds, Brian C O'neill, Shinichiro Fujimori, Nico Bauer, Katherine Calvin, Rob Dellink, Oliver Fricko et al. 2017. "The shared socioeconomic pathways and their energy, land use, and greenhouse gas emissions implications: an overview." *Global Environmental Change* 42:153–168.

Ricke, Katharine, Laurent Drouet, Ken Caldeira, and Massimo Tavoni. 2018. "Country-level social cost of carbon." *Nature Climate Change* 8 (10):895.

Rohde, Robert, Richard Muller, Robert Jacobsen, Saul Perlmutter, Arthur Rosenfeld, Jonathan Wurtele, J Curry, Charlotte Wickham, and S Mosher. 2013. "Berkeley Earth temperature averaging process." *Geoinfor Geostat: An Overview* 1 (2):1–13.

Schlenker, Wolfram and Michael J Roberts. 2009. "Nonlinear temperature effects indicate severe damages to US crop yields under climate change." *Proceedings of the National Academy of Sciences* 106 (37):15594–15598.

Sheffield, Justin, Gopi Goteti, and Eric F Wood. 2006. "Development of a 50-year high-resolution global dataset of meteorological forcings for land surface modeling." *Journal of Climate* 19 (13):3088–3111.

Sherwood, Steven and Qiang Fu. 2014. "A drier future?" *Science* 343 (6172):737–739.

Sherwood, Steven C and Matthew Huber. 2010. "An adaptability limit to climate change due to heat stress." *Proceedings of the National Academy of Sciences* 107 (21):9552–9555.

Solon, Gary, Steven J Haider, and Jeffrey M Wooldridge. 2015. "What are we weighting for?" *Journal of Human Resources* 50 (2):301–316.

Stern, Nicholas. 2006. *The Economics of Climate Change: The Stern Review*. Cambridge University Press.

Taylor, Karl E, Ronald J Stouffer, and Gerald A Meehl. 2012. "An overview of CMIP5 and the experiment design." *Bulletin of the American Meteorological Society* 93 (4):485.

Tebaldi, Claudia and Reto Knutti. 2007. "The use of the multi-model ensemble in probabilistic climate projections." *Philosophical Transactions of the Royal Society of London A: Mathematical, Physical and Engineering Sciences* 365 (1857):2053–2075. URL http://rsta.royalsocietypublishing.org/content/365/1857/2053.

Thomson, Allison M., Katherine V. Calvin, Steven J. Smith, G. Page Kyle, April Volke, Pralit Patel, Sabrina Delgado-Arias, Ben Bond-Lamberty, Marshall A. Wise, Leon E. Clarke, and James A. Edmonds. 2011. "RCP4.5: a pathway for stabilization of radiative forcing by 2100." *Climatic Change* 109 (1):77. URL https://doi.org/10.1007/s10584-011-0151-4.

Thrasher, Bridget, Edwin P Maurer, C McKellar, and PB Duffy. 2012. "Technical note: Bias correcting climate model simulated daily temperature extremes with quantile mapping." *Hydrology and Earth System Sciences* 16 (9):3309–3314.

Tol, Richard S.J. 1997. "On the optimal control of carbon dioxide emissions: an application of FUND." *Environmental Modeling & Assessment* 2 (3):151–163. URL http://dx.doi.org/10.1023/A:1019017529030.

U.S. Environmental Protection Agency. 2016a. "Recommended Income Elasticity and Income Growth Estimates: Technical Memorandum." Tech. rep., U.S. Environmental Protection Agency Office of Air and Radiation and Office of Policy.

———. 2016b. "Valuing mortality risk reductions for policy: A meta-analytic approach." Tech. rep., U.S. Environmental Protection Agency Office of Policy, National Center for Environmental Economics.

Van Vuuren, Detlef P, Jae Edmonds, Mikiko Kainuma, Keywan Riahi, Allison Thomson, Kathy Hibbard, George C Hurtt, Tom Kram, Volker Krey, Jean-Francois Lamarque et al. 2011. "The representative concentration pathways: An overview." *Climatic Change* 109 (1-2):5.

Viscusi, W Kip. 2015. "The role of publication selection bias in estimates of the value of a statistical life." *American Journal of Health Economics* .

Viscusi, W Kip and Joseph E Aldy. 2003. "The value of a statistical life: a critical review of market estimates throughout the world." *Journal of risk and uncertainty* 27 (1):5–76.

WHO. 2018. "Global Health Estimates 2016: Deaths by cause, age, sex, by country and by region, 2000–2016." Tech. rep., World Health Organization.

World Bank. 2020. "World Development Indicators." .

World Inequality Lab. 2020. "World Inequality Database." URL https://wid.world/data/.

Yuan, Jiacan, Michael L Stein, and Robert E Kopp. 2019. "The evolving distribution of relative humidity conditional upon daily maximum temperature in a warming climate." .